Received XX Month, XXXX; revised XX Month, XXXX; accepted XX Month, XXXX; Date of publication XX Month, XXXX; date of current version XX Month, XXXX.

Digital Object Identifier 10.1109/OJCOMS.202X.XXXXXX

A Survey on Advancements in THz Technology for 6G: Systems, Circuits, Antennas, and Experiments

SIDHARTH THOMAS ***(Graduate Student Member, IEEE)***, **JASKIRAT SINGH VIRDI** ***(Graduate Student Member, IEEE)***, **AYDIN BABAKHANI** ***(Senior Member, IEEE)***, **IAN P. ROBERTS** ***(Member, IEEE)***

Department of Electrical and Computer Engineering, University of California Los Angeles, CA 90095 USA

CORRESPONDING AUTHOR: Sidharth Thomas (e-mail: sidhthomas@g.ucla.edu).

ABSTRACT Terahertz (THz) carrier frequencies (100 GHz to 10 THz) have been touted as a source for unprecedented wireless connectivity and high-precision sensing, courtesy of their wide bandwidth availability and small wavelengths. However, noteworthy implementation challenges persist, ranging from limitations in semiconductor device technologies to antenna design and packaging, as well as system-level issues such as high path loss, complex beam management, and regulatory constraints. In this paper, we survey recent advancements on 6G networks using THz frequencies, with a particular emphasis on the 200–400 GHz frequency range and the IEEE 802.15.3d standard. This band offers a compelling balance by providing ample bandwidth for high data-rate communications, while also exhibiting lower atmospheric absorption for longer-range transmission, and can be viably realized using current semiconductor technologies. Unlike other existing surveys in this domain, we provide a comprehensive and holistic overview of THz systems, circuits, device technology, and antennas while also highlighting recent experimental demonstrations of 6G networks using THz frequencies. Throughout this paper, we review the state-of-the-art in 6G network implementation using THz, and call attention to open problems, future prospects, and areas of further improvement in THz communication technologies to fully realize their potential in next-generation wireless connectivity.

INDEX TERMS Terahertz (THz), 6G, IEEE 802.15.3d, THz applications, device technology, circuits, antenna, transceiver architectures.

I. INTRODUCTION

WIRELESS communication has become an indispensable component of contemporary life, with each generation of technological advancement opening the door to a host of novel applications that transform our lifestyles. With commercial 5G systems under deployment, the focus of many wireless researchers has shifted towards developing the sixth generation (6G) of wireless communication [1], [2]. In this pursuit, the forthcoming wave of technological advancement is poised to revolutionize wireless connectivity by offering unprecedented throughput and latency and expanded capabilities such as sensing, tailored to meet the stringent demands of applications of the next decade.

The necessity for 6G technology primarily stems from the global increase in data generation and consumption [3]–[5]. The amount of data traveling across the internet has exponentially grown over the years, and this trend is expected to continue. The International Telecommunication Union (ITU) predicts that by 2030, global mobile traffic volume will be 670 times higher than in 2010, with aggregate mobile data traffic expected to exceed 5 ZB per month [6], [7]. This is illustrated in Fig. 1. The traffic volume per mobile device in 2030 is expected to increase by 50 times from 2010. This surge is primarily attributed to the widespread proliferation of IoT (Internet of Things) devices, ranging from simple household gadgets to advanced industrial sensors, resulting in a massive and ever-growing volume of data. Automation technologies such as digital twins and the adoption of cloud-based machine learning and artificial intelligence across various sectors have further accelerated this trend [8]. As society's dependence on smart devices and connected systems increases, the demand for a more robust and capable

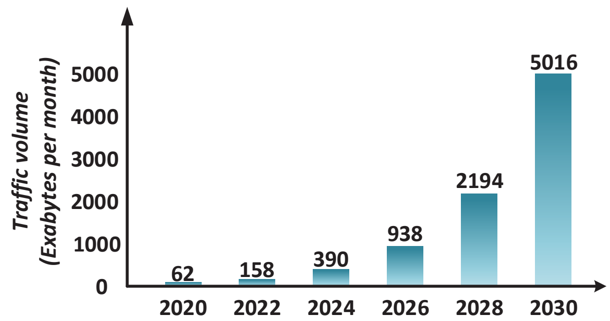

FIGURE 1. The ITU's predicted exponential growth in mobile data traffic through 2030 [6].

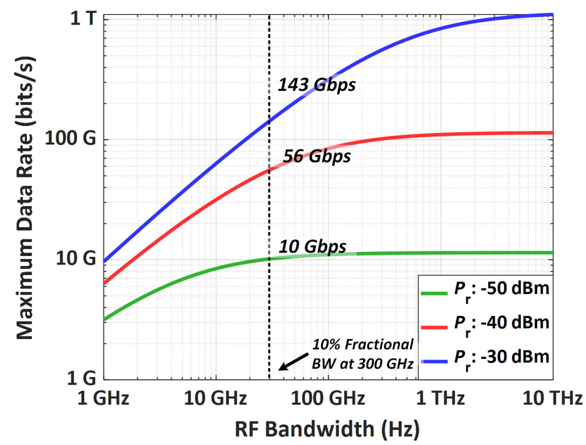

FIGURE 2. The maximum data rate that can be achieved using the Shannon channel capacity theorem plotted against the RF bandwidth for different received powers, P_{r}, assuming a receiver noise figure of 25 dB [30]. The dashed line represents a typical scenario with 30 GHz RF bandwidth, which can be realized by having 10% fractional bandwidth with a 300 GHz carrier.

network infrastructure becomes imperative [9]. In response, 6G aims to deliver speeds, reliability, and latency improvements that far surpass those of its predecessors, establishing a critical foundation for the next era of digital connectivity and innovation. The impressive wireless networks of today are the product of decades of extensive optimization and technology advancements. To deliver future 6G networks which substantially exceed the capabilities of today's 5G networks, many have proposed turning to vast, untapped swaths of spectrum at terahertz (THz) frequencies [10]–[21].

The THz band, which ranges from 0.1 to 10 THz [22]–[24], occupies a distinctive spot in the electromagnetic (EM) spectrum. Positioned between radio frequencies (RF) and optical frequencies, this band displays characteristics of both and offers exciting possibilities for new applications. The THz band can support high-capacity wireless links due to its vast bandwidth availability. Additionally, its short wavelength allows for operating large-scale antenna arrays in a small form factor, enabling improved beamforming, increased coverage, and spatial multiplexing, which facilitates network densification. THz is also ideal for sensing applications, with THz radars and imagers providing superior range and lateral resolution compared to their low-frequency counterparts [25], [26]. Moreover, THz imaging technologies may offer safer, more accessible medical diagnostics than traditional X-ray imaging [27]. These unique features also enable future 6G technologies to combine communication and sensing into a single system, revolutionizing everyday interactions, transforming healthcare, and forging new markets. Table 1 outlines these envisioned applications of THz communications in 6G.

The maximum data rate for a wireless channel with bandwidth B and some signal-to-noise ratio (SNR) can be calculated using the well-known Shannon channel capacity

$$R = B \cdot \log_2(1 + \mathsf{SNR}). \tag{1}$$

While this expression does not strictly depend on carrier frequency, bandwidth availability tends to increase at higher carrier frequencies [28], [29]. Increasing bandwidth B then facilitates higher data rates, assuming there is sufficient SNR to meet bit-error-rate requirements. For instance, at 300 GHz, the maximum data rate for a link with a 25 dB noise figure (representative number [30]) is plotted in Fig. 2 for various received power levels. With a 10% fractional bandwidth (i.e., $B = 30$ GHz) and -40 dBm received power, a link can support an astonishing 56 Gbps. Such massive bandwidths also introduce the potential to multiplex an unprecedented number of devices across time and frequency, with each device enjoying substantial data rates.

A few THz bands in particular have garnered substantial interest for their applications in wireless communication. These bands include the D-band (110–170 GHz) [10]–[12], the 300 GHz band (253–322 GHz) [13]–[18], and the 400 GHz band [19], [20]. Operating at these THz frequencies presents unique challenges spanning various technical considerations such as device technology, circuit design, antenna design, packaging, channel modeling, signal processing, and system design [7], [30]. These complexities associated with realizing THz transceivers and deploying THz wireless systems has drawn considerable attention and investment from both industrial and academic research laboratories. This has led to several standardization efforts for THz bands [31], [41], [60]–[62], with perhaps the most notable being IEEE 802.15.3d [62]. This standard ultimately seeks to enable wireless communication over channels as wide as 69 GHz within the 253–322 GHz frequency range [41]. Its primary aim is to showcase the feasibility of THz frequencies for communication. Additionally, it serves as a coordinated effort toward developing effective and reliable connectivity solutions at THz.

In this paper, we survey several key techniques and technologies for enabling wireless communication at carrier frequencies beyond 200 GHz and focus in particular on current specifications of the IEEE 802.15.3d standard. In this pursuit, we conduct a comprehensive analysis of the latest developments, potential opportunities, challenges, and the current

TABLE 1. Noteworthy Applications of THz Communication in 6G

Application	Description
High-speed data transfer and connectivity	• WLAN: Enhanced hotspots for high-speed wireless data transfer [22], [31] • IoT: Large-scale connectivity with edge intelligence [32] • Kiosk downloading: "Touch-and-go" transfer of massive files [33] • High-speed trading applications for financial hubs [34]
Wireless backhaul	• Cost-effective alternative to fiber for mm-Wave base stations [35]–[37] • Facilitates computing and cloud-based services such as AI and digital twins at the network's edge [38]
AR/VR and holographic projections	• Enables a high-capacity, low-latency link that can facilitate computational offloading from AR/VR headsets, allowing them to reduce their form factor and battery consumption [39] • Enables healthcare applications including remote surgery [40]
Data centers	• Flexible, cost-effective alternative to Ethernet and fiber [41] • Reduced latency compared to optical fiber [42]
Joint communication and sensing (JCAS)	• Leverages existing communication infrastructure for wide area sensing while improving communication system performance through dynamic adjustments [43] • Applications in industrial automation, robotics, and AR/VR, and can enable real-time digital twins and autonomous driving [44]
Secure communication	• Inherent security features: – Highly directional nature reduces eavesdropping risk [9] – "Whisper radio" concept leverages high signal attenuation for localized, secure communication [45] • Advanced modulation schemes enhance physical layer security: – Space-time modulated phased arrays (Fig. 3 (a)): Parallel data streams are modulated spatially and temporally, allowing deciphering by intended broadside receivers while corrupting signals for off-axis eavesdroppers [46] – Orbital Angular Momentum (OAM) (Fig. 3 (b)): Information is modulated on carrier signals with specific angular momentum modes, ensuring only receivers with matching modes can decipher it [47], [48]
Satellite communication	• Viable for ground-satellite links due to reduced atmospheric attenuation at higher altitudes [49] • Outperforms optical links in inter-satellite communication with broader, more reliable beams [49] • Lower power consumption and weight compared to laser-based systems [30], [50]
Autonomous Vehicles	• Should meet the stringent vehicular communication requirements: ultra-high reliability (>99.9999%), ultra-low latency (<1ms), and performance at high speeds (up to 1000 km/h) [8] • Complements existing data transfer methods and enables interconnected sensor networks for seamless communication, enhancing safety and efficiency in autonomous driving systems [51]

state-of-the-art in the 200–400 GHz range. Unlike other existing surveys in this domain ([1], [7], [22], [24], [52]–[59]), this work offers a comprehensive and holistic overview of THz systems, circuits, device technology, and antennas, while also emphasizing recent experimental demonstrations of 6G networks using THz frequencies (Table 2). We describe the unique challenges in these areas specific to THz design, acknowledge the limitations of current technology, and highlight promising approaches for practical solutions. Furthermore, we provide an overview of notable demonstrations of 6G systems operating at THz frequencies across the globe and examine their architectural and implementation considerations, a crucial step to hone in on capable, cost-effective THz systems for future commercial 6G systems.

The rest of this paper is organized as follows. Section II reviews the nature of wireless propagation channels at THz frequencies. Section III describes the IEEE 802.15.3d standard. Section IV surveys the state-of-the-art in semiconductor device technology. Circuit techniques and architectures suited for THz design are discussed in Section V. Antenna design and packaging techniques are addressed in Section VI. Section VII showcases notable THz demonstrations worldwide. Section VIII highlights some of the open research areas in realizing 6G systems using THz. Finally, the paper is concluded in Section IX, summarizing the key findings and insights of this survey. Table 3 summarizes key acronyms used throughout this paper. Fig. 4 outlines the organization of this survey.

TABLE 2. Comparison of Surveys on THz Communication

Reference	Year	Content					
		6G & Applications	THz Channel	Devices	Circuits	Antennas & Packaging	Demos
Rappaport et al. [1]	2019	✓	✓	✗	✗	✗	✗
Tekbıyık et al. [52]	2019	✓	✓	✓	✗	✓	✗
Chen et al. [53]	2019	✗	✗	✓	✗	✓	✓
Chowdhury et al. [7]	2020	✓	✗	✗	✗	✗	✗
Elayan et al. [24]	2020	✓	✓	✓	✗	✗	✗
He et al. [54]	2020	✗	✗	✗	✗	✓	✗
Lemic et al. [55]	2021	✓	✓	✗	✗	✗	✗
Wang et al. [56]	2021	✓	✓	✗	✗	✓	✗
Akyildiz et al. [22]	2022	✓	✓	✓	✗	✓	✗
Han et al. [57]	2022	✗	✓	✗	✗	✗	✗
Serghiou et al. [58]	2022	✓	✓	✗	✗	✗	✗
Jiang et al. [59]	2024	✓	✓	✓	✗	✓	✓
This work	2025	✓	✓	✓	✓	✓	✓

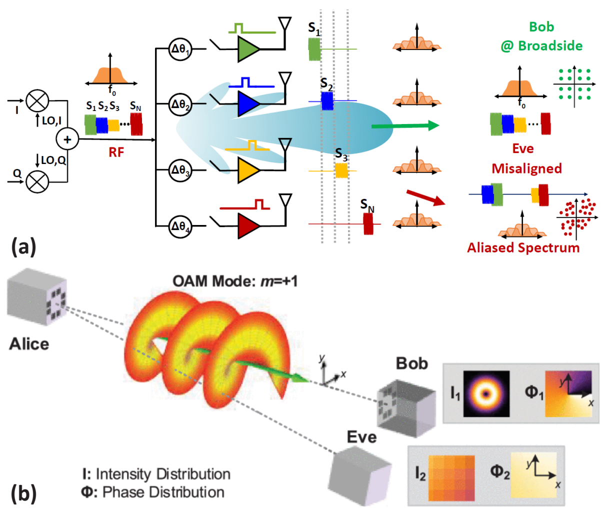

FIGURE 3. (a) Application of a space-time modulated phased arrays in transmitting data selectively towards the intended receiver, Bob, while corrupting the data constellation and spectrum towards the eavesdropper, Eve [46]. (b) A THz OAM transceiver can establish a physically secure wireless link that is resistant to off-beam-axis eavesdropping. Here, Bob, the intended receiver, operates in the same mode as Alice and can receive the information. The eavesdropper, Eve, is off-axis and cannot receive information [47].

II. WIRELESS CHANNEL CHARACTERISTICS

Wireless channels at THz bands exhibit behaviors markedly distinct from other key frequencies, such as sub-6 GHz bands and mm-Wave bands. This difference arises from the unique interaction between EM waves and materials at THz frequencies, whose dynamics are heavily dependent on the wavelength relative to the physical dimensions of the objects it interacts with. THz channels show high levels of signal attenuation and display scattering properties notably different from their lower-frequency counterparts, and they exhibit strong absorption loss, susceptibility to blockage, and shadowing [1], [2]. This results in a sparse channel with few paths from the transmitter to the receiver, which can lead to reliability concerns in certain applications and environments.

A. Path Loss

Similar to traditional wireless systems, the path loss in THz systems primarily stems from free-space path loss (FSPL) and atmospheric attenuation, each characterized by distinct mechanisms as outlined below.

1) Free-Space Path Loss

FSPL occurs from the radial spread of EM waves as they travel through free space. This is famously quantified by

$$L = \left(\frac{4\pi d}{\lambda}\right)^2, \tag{2}$$

where L represents the path loss, d signifies the distance the wave has propagated, and λ is the wavelength of the EM wave [42]. Note that the antenna gain can be embedded along with FSPL. The FSPL with isotropic antennas at 3 GHz, 30 GHz, and 300 GHz are plotted with dashed lines in Fig. 5(a). It can be observed that the path loss worsens at higher frequency. As we shall see shortly, this trend reverses when the physical aperture of the antenna is fixed.

2) Atmospheric Attenuation

THz frequencies experience higher atmospheric attenuation than RF frequencies due to various effects. THz wavelengths are comparable in size to dust, rain, snow, and other atmospheric particles, which leads to higher attenuation [1]. Moreover, several absorption resonances exist at THz frequencies, which occur when the frequency approaches the energy required to excite vibrational modes in molecules. The THz absorption spectrum is plotted in Fig. 6 for standard (blue) and dry (red) atmospheric moisture conditions.

TABLE 3. List of Acronyms

5G	Fifth generation of wireless communication
6G	Sixth generation of wireless communication
BiCMOS	Bipolar CMOS
BPSK	Binary phase shift keying
CMOS	Complementary metal-oxide-semiconductor
DS	Directive scattering
EM	Electromagnetic
FDSOI	Fully depleted silicon on insulator
FSPL	Free-space path loss
$f_{\max}$	Maximum oscillation frequency
f_{T}	Transit frequency
GaAs	Gallium arsenide
HBT	Heterojunction bipolar transistor
HEMT	High-electron-mobility transistor
IC	Integrated circuit
InP	Indium phosphide
IoT	Internet of things
ITU	International telecommunication union
JCAS	Joint communication and sensing
LNA	Low-noise amplifier
LO	Local oscillator
LDPC	Low-density parity-check code
M-QAM	M-ary Quadrature amplitude modulation
MIMO	Multiple input multiple output
OAM	Orbital angular momentum
OOK	On-off keying
OTA	Over-the-air
PA	Power amplifier
PCB	Printed circuit board
QPSK	Quadrature phase shift keying
RIS	Reconfigurable intelligent surface
SiGe	Silicon-germanium
SNR	Signal-to-noise ratio
THz	Terahertz
THz-OOK PHY	Terahertz on-off keying physical layer
THz-SC PHY	Terahertz single carrier physical layer
WLAN	Wireless local area network

Sharp absorption peaks are observed at 183 GHz, 325 GHz, 380 GHz, and 450 GHz, which arise due to rotational and vibrational excitation states in gas molecules [63]. While these bands have some applications in short-range secure communication schemes such as "whisper radio" [45], and in applications such as hydration sensing and spectroscopy [64], [65], they should generally be avoided for long-distance communication. Note that some frequency bands, such as the D-band (110-170 GHz), 300 GHz, and 400 GHz bands, do not have significant absorption peaks. As a result, these frequencies are optimal candidates for 6G networks using THz. At 300 GHz, for instance, the atmospheric attenuation is as low as 10 dB per km, a tolerable level for communication links [1], [63].

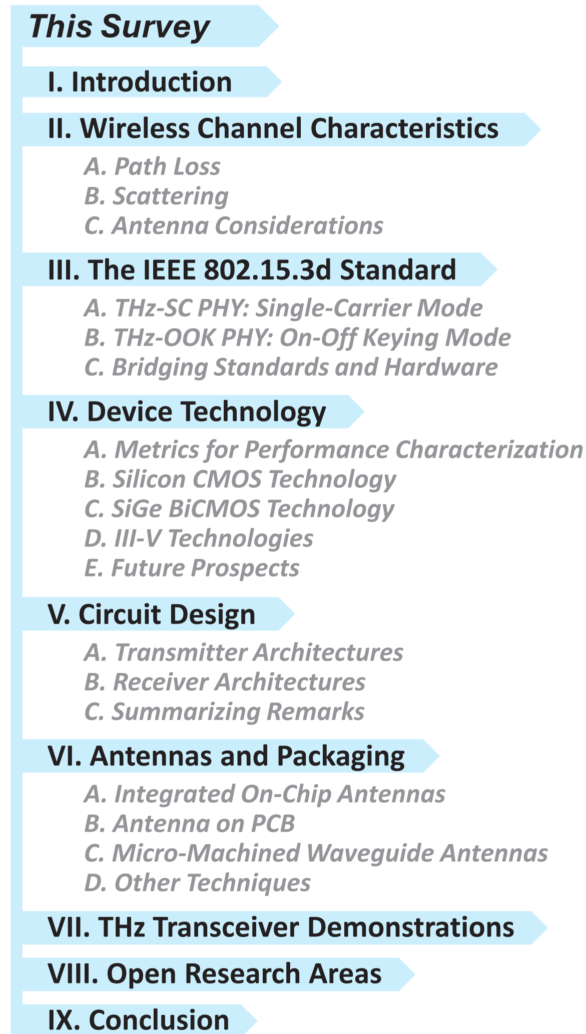

FIGURE 4. Organization of this survey

B. Scattering

The scattering behavior of an EM wave with a material depends on the roughness of the scatterer with respect to the wavelength [45]. In quantifying this, the Rayleigh criterion can be used to determine the smoothness or roughness of a surface [66]. It defines a critical height of a surface, h, which depends on the wavelength and the angle of incidence, θ_i. The critical height is given by

$$h = \frac{\lambda}{8 \cos \theta_i}. \tag{3}$$

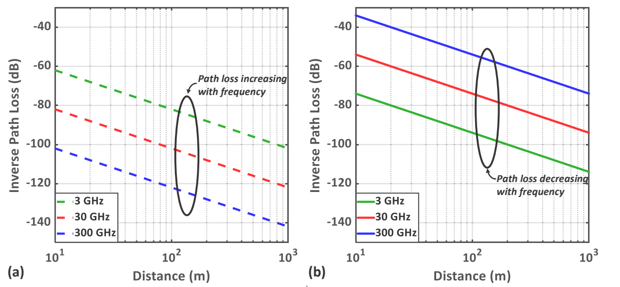

FIGURE 5. Inverse path loss, $(1/L)$, versus distance for different frequencies. Note that the antenna gain is embedded with the loss. (a) The dashed line represents the loss with an isotropic antenna. The path loss increases with frequency for a given distance. (b) The solid line represents the loss with a directive antenna (having a fixed physical aperture for all three frequencies). In this case, the path loss decreases with frequency for a given distance.

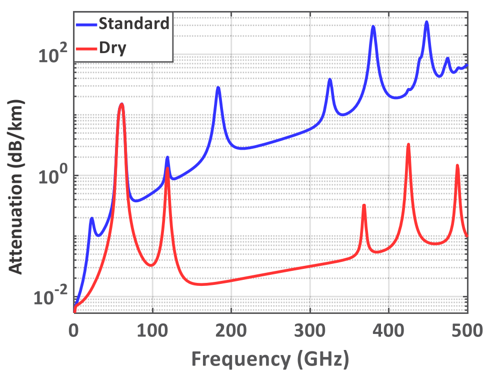

FIGURE 6. Atmospheric attenuation versus frequency in standard (blue) and dry (red) conditions [63]. Strong absorption bands can be observed at 183 GHz, 325 GHz, 380 GHz, and 450 GHz.

The surface is considered smooth for a given frequency with wavelength λ if the minimum to the maximum surface protuberance, h_0, is smaller than h. At RF frequencies, most surfaces are smooth and follow reflection-like specular behavior, in which case, the reflection process has a strong dominant specular path, where the incident angle equals the reflected angle. There is also little absorption. This results in a rich multi-path channel that can be studied with several models. At optical frequencies, the scattering is diffuse, with multiple signal paths across different directions (Fig. 7).

The channel behavior is much different at THz. Here, the surface roughness of many everyday objects becomes comparable to the wavelength, and hence, scattering shows both diffuse and specular behavior (Fig. 7) [1]. This results in many scattered waves in addition to the primary reflected specular component, resulting in multiple signal paths spread across different directions. This is studied using the directive scattering (DS) model in [67], which shows that the scattered power is higher at higher frequencies relative to the specularly reflected power. Interestingly, the strongest scattering happens when the wave hits the surface straight on. However, when the wave grazes the surface, the scattering sharply decreases, and most of the wave's energy is instead reflected [67].

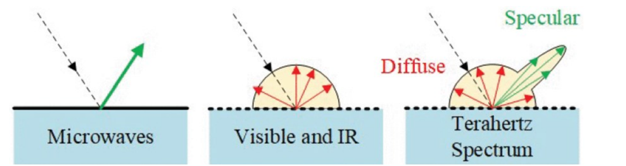

FIGURE 7. Surface scattering exhibiting specular behavior for microwaves, diffuse behavior for visible and infrared frequencies, and a combination of both for THz frequencies [1]

C. Antenna Considerations

In order to compensate for the increased path loss and attenuation at THz frequencies, highly directive antennas are often required and this naturally results in a communication link which is highly directional. This contrasts with lower frequencies, where conventional cellular antennas can broadcast over a wide coverage angle [29], [68]. This stark difference in the directionality of transmission introduces noteworthy challenges at high carrier frequencies, as already observed in mm-Wave 5G.

A large-scale phased array is perhaps the ideal way to realize high directivity. A linear N-element half-wavelength antenna array offers an increase in directivity, which scales in dB as $10\log_{10}(N)$ [69], by forming highly directive beams. The ability of phased arrays to electronically steer their beams (as opposed to mechanically) makes them preferred in most 6G use cases in order to overcome blockage that may arise and to serve many users. Using a multi-antenna architecture also makes it possible to perform MIMO techniques such as spatial multiplexing, potentially across users, to increase data rates [70], [71]. It should be noted that beamforming should ideally be realized using true-time delays rather than phase shifters to avoid beam squint, which can become prominent in THz communication, where channels may consume a large fractional bandwidth [72]. MEMS-based mechanical steering is also being actively investigated as another possible solution [73], though this would likely be most useful for point-to-point links where channel variations are slow.

High directivity can also be realized using passive structures such as a lens antenna or a parabolic reflector [74]. This approach becomes advantageous at THz frequencies since higher frequencies result in greater antenna directivity, given a specific aperture area [69]. For an antenna with an aperture area of A_e, the antenna gain, G_a, is given by

$$G_\mathrm{a} = \frac{4\pi A_\mathrm{e}}{\lambda^2}. \tag{4}$$

This equation suggests that A_e increases with frequency for a given aperture. Using such an antenna at the transmitter and receiver, the overall channel loss, L, is given by (5) after embedding the antenna gain.

$$L = \left(\frac{\lambda d}{A_\mathrm{e}}\right)^2 \tag{5}$$

It can be observed that the channel loss now decreases with an increase in frequency. This is plotted in Fig. 5(b) using the solid lines for an A_e of 2 cm^2. THz link budgets can thus outperform RF link budgets, in theory, for a given antenna aperture at the transmitter and receiver.

When employing an antenna whose aperture is large relative to the wavelength, it is essential to begin considering the far-field distance [69]. The minimum distance to the far-field region, d_far, for an antenna with a maximum dimension of D and wavelength of λ is given by

$$d_\mathrm{far} = \frac{2D^2}{\lambda}. \tag{6}$$

Due to the small wavelengths, the far-field distance can become quite substantial at THz frequencies, even for modest apertures. For instance, employing a 10 cm antenna array can result in a far-field distance of 20 m at 300 GHz. This sizable distance indicates that a receiver may likely operate in the near-field, necessitating a redesign of conventional beam-steering algorithms [9]. For example, [75] proposes performing wavefront engineering for link maintenance, where so-called "airy" beams are created to curve around potential blockages in the near-field.

It is worth noting that while highly directional beams may indeed be formed at THz using the aforementioned methods, a key challenge remains in efficiently closing and reliably maintaining the link between two devices [76]. The overhead of traditional mmWave beam sweeping approaches to close the link may be unsuitable at THz, as beams are even more narrow and path loss is even more severe. This necessitates new mechanisms and procedures for beam management in order to ensure that communication between two devices can be established and maintained.

Beam management, encompassing initial access and beam tracking, is crucial for robust mmWave and THz communications, especially in mobile scenarios [77]. The narrow beams at higher frequencies exacerbate link establishment challenges and lead to significant beam measurement overhead, impacting beam acquisition and tracking. Channel fluctuations, user mobility, and environmental changes further complicate these issues. Emerging technologies like artificial intelligence and reconfigurable surfaces are being explored to address beam management challenges in mmWave and THz communications [77]–[80].

III. THE IEEE 802.15.3d STANDARD

The IEEE 802.15 Terahertz Interest Group was established in 2008 to explore wireless communication within 0.3 to 3 THz. In 2017, the IEEE 802.15.3d standard (the 300 GHz band) was approved, serving as an initial step towards THz communication [62]. This standard outlines a PHY layer of 100 Gbps, with the option to revert to lower rates. It supports

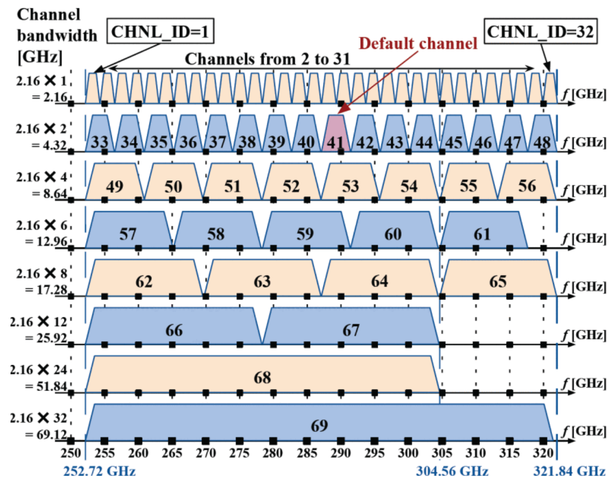

FIGURE 8. Channel plan for the IEEE 802.15.3d standard [41]. There are 69 overlapping channels between 252.72 GHz and 321.84 GHz, which support 8 channel bandwidths from 2.16 GHz up to 69 GHz.

wireless communications over channels as wide as 69 GHz within 253–322 GHz. The primary goal of this standard is to demonstrate the practicality of using THz frequencies for communication. Note that the envisioned applications are restricted primarily to point-to-point links between static or quasi-static devices, to remain within the realm of what is possible with current semiconductor technology. However, this may change in the future as device technology matures. A detailed description of this standard can be found in [41].

As illustrated in Fig. 8, the IEEE 802.15.3d standard covers frequencies between 252.72 GHz and 321.84 GHz, with 69 overlapping channels. These channels offer eight supported bandwidth options, ranging from 2.16 GHz to 69.12 GHz, each bandwidth being an integer multiple of 2.16 GHz. Channel number 41 is used by default, with a bandwidth of 4.32 GHz. Summarized next, the PHY layer in the IEEE 802.15.3d standard has two modes: THz single-carrier mode (THz-SC PHY) and THz on-off keying mode (THz-OOK PHY).

A. THz-SC PHY: Single-Carrier Mode

THz-SC PHY aims to achieve high data rates and caters to bandwidth-oriented use cases such as wireless fronthaul/backhaul and data center links. This mode offers a range of six different modulations, including four variations of phase-shift keying: binary (BPSK), quadrature (QPSK), 8-phase (8-PSK), and 8-phase asymmetric (8-APSK). In addition, quadrature amplitude modulation (QAM) is available as 16-QAM and 64-QAM. While BPSK and QPSK modulations are mandated for the THz-SC mode, support for other modulations are optional. This mode employs one of two low-density parity check (LDPC) codes for forward error correction: a high-rate 14/15 LDPC (1440, 1344) or a low-rate 11/15 LDPC (1440, 1056).

B. THz-OOK PHY: On-Off Keying Mode

THz-OOK PHY mode is designed to cater to low-complexity THz devices by using low-cost, relatively simple amplitude modulation schemes. Despite this limitation, it can still attain impressive data rates of up to tens of gigabits per second when utilizing the widest channels available. In terms of coding, three different error correction schemes are supported, including the mandatory (240, 224)-Reed Solomon code for simple hard decoding. Additionally, the two LDPC-based schemes described in the previous subsection can also be used with THz-OOK operation for soft decoding.

C. Bridging Standards and Hardware: The Path Forward

The IEEE 802.15.3d standard marks a significant milestone in THz communication, outlining the framework to achieve high-speed wireless links in the 300 GHz band. However, translating this standard into practical, commercially viable systems presents challenges that span multiple domains. Several critical areas require focused research and development:

1) Device Technology: Transistors capable of efficient operation at THz frequencies while remaining cost-effective are crucial.
2) Circuit Architectures: Innovative circuit designs are needed to overcome device limitations and optimize performance within the constraints of available technologies.
3) Packaging and Antennas: The short wavelengths at THz frequencies necessitate novel approaches to packaging and antenna design. These components must not only meet performance requirements but also remain economically viable for mass production.

Bringing together devices, circuits, and antennas into cohesive, reliable systems that meet the standard's specifications is a complex task requiring interdisciplinary expertise. Generating signals in an energy-efficient manner at the frequencies specified by the standard is challenging. Moreover, the standard requires broadband operation, which is difficult due to imperfections in devices, circuits, packaging, and antennas. Additionally, implementing higher-order modulation schemes, such as 16-QAM and 64-QAM, for THz-SC mode, places stringent demands on the noise and non-linearity performance of the hardware. The following sections will delve into these critical areas while highlighting both the progress made and the challenges that lie ahead in bridging the gap between the IEEE 802.15.3d standard (and future standards) and commercially viable THz communication systems.

IV. DEVICE TECHNOLOGY

This section compares key semiconductor technologies suitable for designing circuits in the IEEE 802.15.3d band. "Technology" or a "process" in this context refers to a specific semiconductor manufacturing process and its feature size. Examples of this include silicon CMOS (complementary metal-oxide-semiconductor), SiGe BiCMOS (Silicon-Germanium Bipolar CMOS), and III-V technologies like InP (Indium Phosphide) and GaAs (Gallium Arsenide) [81]. Table 4 provides an overview of this comparison.

TABLE 4. Comparison of Various Device Technologies

Device Technology	Silicon CMOS	SiGe BiCMOS	III-V Semiconductors
Active Devices	FET	HBT	HBT, HEMT
Peak f_{max} (GHz)	~ 370 (at 22nm)	~ 720	> 1000
PA Output Power	Low	Moderate	High
Monolithic Digital Integration	Excellent	Moderate (Slow Digital)	Not Possible
Cost	Low	Moderate	High

A. Metrics for Performance Characterization

A key challenge in THz circuit design stems from the limitations in transistor performance [82]. At these frequencies, transistor performance degrades to the point where it can no longer provide amplification. Furthermore, the interconnects that allow for electrical connections to the transistor add significant parasitic resistance, capacitance, and inductance, further hindering overall performance. Transistors also exhibit non-quasistatic behavior at THz frequencies, making their modeling complicated.

A technology-agnostic metric commonly used to characterize the transistor performance at high frequencies is the maximum oscillation frequency, $f_{\max}$. For any 2-port device (such as a transistor), $f_{\max}$ is the frequency at which the maximum available power gain (or the unilateral power gain) drops to zero [42]. In other words, amplifiers and oscillators cannot be built beyond the $f_{\max}$ of a technology.

In general, circuit design becomes challenging beyond $f_{\max}/2$. Amplifiers operating at these frequencies require several stages to attain even modest levels of amplification. Consequently, power amplifiers at these frequencies have low saturated output power and low power-added efficiency, and low-noise amplifiers have high noise figures, both of which are detrimental to transceiver performance. A higher $f_{\max}$ almost always implies a better communication link for the same DC power, enabling more energy-efficient communication. It should be noted that, while amplification is not possible beyond $f_{\max}$, generating signals using non-linear circuit design techniques is possible. However, these techniques usually have low efficiencies ($<0.5\%$) [83]. This will be discussed later in Section VI.

The transit frequency, f_{T}, is another metric for high-frequency technology characterization. It is the frequency at which the current gain of a transistor, with source and drain shorted, drops to unity. While the relative importance of the two parameters is debated, $f_{\max}$ is often seen as a better metric for high-frequency characterization. This is because f_{T} does not account for important non-idealities such as the gate resistance, which degrades high-frequency device

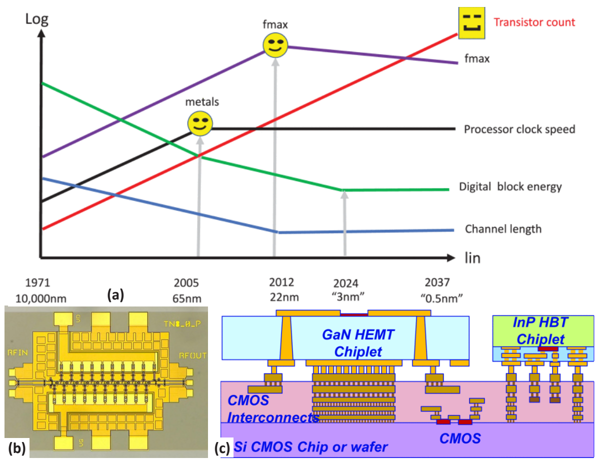

FIGURE 9. (a) Illustration of CMOS scaling, with asymptotic development following Moore's law. While the transistor count has remained increasing over the years, $f_{\max}$ peaked at 22nm [85]. (b) First demonstration of a 1 THz amplifier using InP [86]. (c) Example demonstrating "best junction for the function" through heterogeneous integration [87].

performance [84]. For this reason, we will emphasize $f_{\max}$ as a standard for comparing technologies throughout this survey.

B. Silicon CMOS Technology

Silicon CMOS is the most popular choice when designing integrated circuits. This is mainly due to its low cost and high digital integration capabilities, enabling systems-on-chip (SoCs) with enhanced sensing and computing capabilities. A CMOS technology node is characterized by its feature size, which roughly describes the smallest dimension of the transistor gate length. For example, a 65nm CMOS node offers CMOS transistors with a minimum gate length of 65nm. Note that this naming convention is not strictly followed in recent technology nodes.

CMOS technology has rapidly scaled to lower dimensions for the past several decades, famously following Moore's law, resulting in an exponential growth in computing capabilities. However, since this scaling has been driven by a desire to enhance digital CMOS performance, it has not necessarily translated to enhanced RF performance [85]. This behavior is illustrated in Fig. 9(a), where different transistor performance metrics are plotted for various technology nodes. Notice that the transistor count has increased exponentially and is accompanied by a reduction in digital block energy, pushing Moore's law forward. However, $f_{\max}$ reached its peak at 22nm, with an $f_{\max}$ of 370 GHz [88]. While $f_{\max}$ generally increases with channel length reduction due to shorter transit times and lower intrinsic capacitances, further scaling below 22nm introduces significant resistive losses in interconnects, leading to a decline in $f_{\max}$. This trend is concerning for THz circuit designers since they can no longer rely on technology scaling to push to higher frequencies. This demands new circuit design techniques or switching to a non-CMOS platform.

C. SiGe BiCMOS Technology

The SiGe BiCMOS process is another popular choice for THz circuit design, as it provides high-performance HBTs (heterojunction bipolar transistors). These processes often utilize the same platform as a CMOS node, thereby inheriting the benefits associated with digital CMOS technology. Cutting-edge SiGe processes have achieved an $f_{\max}$ reaching up to 720 GHz [89]. However, it is essential to acknowledge that the CMOS transistors integrated within these nodes are typically from earlier generations. This makes it difficult to integrate complex digital processing into the same chip. For instance, the most advanced BiCMOS process currently offers CMOS transistors with a 45nm feature size, a technology that is over a decade old [90].

D. III-V Technologies

III-V semiconductors, such as gallium arsenide (GaAs) and indium phosphide (InP), present numerous benefits over conventional silicon-based technologies. These advantages stem from higher electron mobility, higher breakdown voltages, and improved high-temperature performance. In particular, InP HBTs and HEMTs (high-electron-mobility transistors) are among the most favored III-V technologies for THz circuit design, capable of reaching an $f_{\max}$ beyond 1 THz [91], [92]. For example, Northrop Grumman has showcased a 1 THz amplifier in InP, as detailed in [86] (Fig. 9(b)). Despite these advantages, III-V technologies have not been as widely adopted as CMOS and SiGe due to their higher costs, lack of digital integration capabilities, and smaller available wafer sizes [82]. However, with the advent of 6G and the push to higher carrier frequencies, III-V semiconductor technology could significantly grow in demand and maturity, addressing some of these challenges.

E. Future Prospects

Significant research efforts are underway to enhance device performance, highlighted by initiatives like DARPA's T-MUSIC program in North America [93] and the TARANTO project in Europe [94]. For circuit design in the THz band, adopting a "best junction for the function" strategy is often recommended (Fig. 9(c)) [87]. This strategy integrates advanced III-V technologies for the RF front-end with CMOS technology for digital components. Achieving this integration depends on advancements in packaging techniques and heterogeneous integration [95], [96].

Resonant tunneling diodes [97], traveling wave tubes [98], and photonic techniques like quantum cascade lasers [99] have also been explored for generating THz signals. These advanced technologies offer promising avenues for THz applications but face high costs, complex fabrication processes, and integration and scalability issues [81]. Despite these challenges, ongoing research aims to improve their accessibility and compatibility with existing semiconductor processes, potentially paving the way for their increased role in future THz systems.

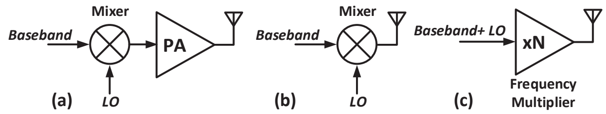

FIGURE 10. **Transmitter architectures suitable at THz frequencies: (a) PA-last transmitter (b) Mixer-last transmitter (c) Multiplier-last transmitter**

V. CIRCUIT DESIGN

Circuit design techniques at THz frequencies differ notably from those used for RF and mmWave frequencies. This is primarily because of the degradation in transistor performance due to the limited $f_{\max}$ [100]. Additionally, passive devices such as capacitors and inductors suffer from a high loss at these frequencies due to the skin effect, self-resonance, and substrate coupling. Due to these limitations, designing amplifiers, local oscillators (LOs), and frequency synthesizers at THz frequencies has proven difficult.

Harmonic techniques play a significant role in circuit design at these frequencies. Any non-linear system generates higher-order harmonic products when driven by a large-signal input. Conventionally, these harmonic products are undesired and need to be removed. However, these harmonics can prove useful at THz circuit design to generate signals beyond $f_{\max}$. The greater the non-linearity, the stronger the higher-order harmonics, resulting in greater THz signal efficiency.

Consider a non-linear device, such as a transistor, driven by an RF source. Strong harmonic products are generated if the source power is large enough to drive this device into non-linear operation. When an NMOS transistor is driven by a voltage V_{in} at frequency f_0, the drain current I can be expressed as

$$I = I_0 + g_{m1}V_{\text{in}} + g_{m2}V_{\text{in}}^2 + g_{m3}V_{\text{in}}^3 + \cdots , \qquad (7)$$

where I_0 represents the DC, while $g_{m1}V_{\text{in}}$ represents the output current at f_0 [101]. The output current includes higher-order terms generated due to transistor non-linearity, which are represented by $g_{m2}V_{\text{in}}^2$ and $g_{m3}V_{\text{in}}^3$. These terms contain harmonic signals at $2f_0$ and $3f_0$, respectively. These higher-order harmonic terms can be extracted and used to design THz signal sources. Note that while non-linearity can be used to design signal sources and synthesizers beyond $f_{\max}$, it still cannot achieve amplification.

Extensive research is underway within the circuit design community to improve the performance of transmitters, receivers, and local oscillators for THz operation. This section overviews various transmitter and receiver architectures for THz circuit design. Understanding trade-offs within various architectures is crucial in choosing the correct modulation schemes to maximize data rates and spectral efficiency.

A. Transmitter Architectures

We now highlight various transmitter architectures that are feasible at THz frequencies, as shown in Fig. 10.

1) PA-Last Architecture

Fig. 10(a) shows the conventional transmitter architecture which is used at RF frequencies, where a PA is followed by an antenna. This architecture can support both amplitude and phase modulation schemes by incorporating a linear power amplifier as its final stage, enabling higher-order modulation schemes like M-QAM. However, due to the aforementioned $f_{\max}$ limitations of PAs, several amplification stages are needed to achieve sufficient amplification at THz frequencies. This impacts power consumption, amplifier stability, and efficiency [17]. For instance, [102] demonstrates a 290 GHz power amplifier in a 130nm BiCMOS process with a saturated output power of 7.5 dBm and a power added efficiency of just 0.39%. (Power added efficiency is the ratio of the difference of the output and input signal power to the DC power consumed.) Because of this, PA-last techniques are usually avoided while designing in CMOS/SiGe platforms, which have a lower $f_{\max}$. However, this architecture remains popular in InP transmitters [103], which have a relatively high $f_{\max}$.

2) Mixer-Last Architecture

This architecture does not use a power amplifier at all, and instead, the final stage features a mixer, as seen in Fig. 10(b). A mixer behaves linearly for the input baseband signal but has non-linear behavior with the LO [16] and thus performs upconversion. Conventionally, the baseband signal is upconverted to the LO frequency. However, an N-th harmonic mixer can be designed, which upconverts the baseband signal to the N-th harmonic of the LO. This approach is capable of operating at frequencies beyond $f_{\max}$ and has been utilized in [14] and [13] with the second and third harmonics of the LO, respectively. This topology can support M-QAM modulation as the mixer behaves linearly and maintains the amplitude and phase information of the input baseband signal. However, mixers typically provide low-output saturated power, which affects the link budget and can thus limit the modulation order and viable link distance.

3) Multiplier-Last Architecture

Shown in Fig. 10(c), this architecture utilizes a frequency multiplier as the final stage. A frequency multiplier is a circuit designed to maximize non-linearity to achieve high output power at a particular harmonic of the input. Frequency multipliers typically can achieve higher output power than a mixer and have seen some success in THz transceiver design [19], [20], [104]. However, this technique has a few noteworthy challenges.

Firstly, amplitude distortion can occur due to the inherently non-linear nature of frequency multiplication. This makes it difficult to support higher-order amplitude modulation schemes (i.e., modulation involving more than two amplitude levels). Secondly, phase distortion can also occur

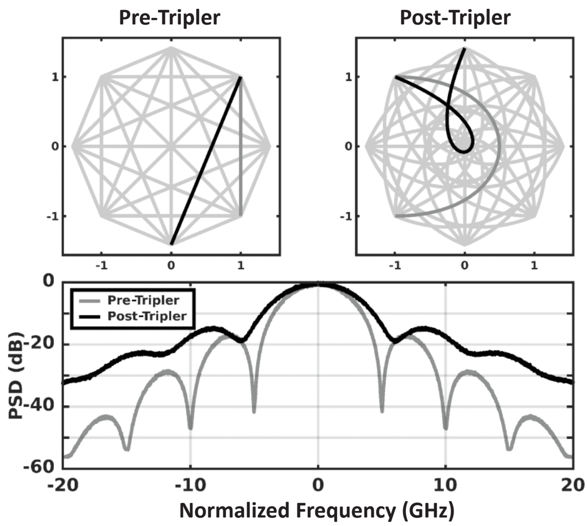

FIGURE 11. Constellation diagrams and spectrum for an 8PSK signal pre-and post-tripling [20]. Constellation points change their position post-tripling. However, they do not fall over each other and cause signal corruption. In the frequency domain, bandwidth expansion takes place post-tripling.

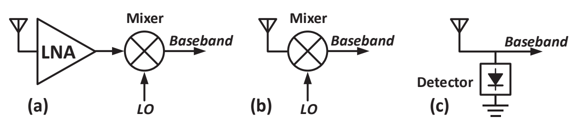

FIGURE 12. Receiver architectures suitable at THz frequencies: (a) LNA-first receiver (b) Mixer-first receiver (c) Power detector based receiver

during frequency multiplication, causing constellation points to rotate. For instance, an 8PSK signal upon doubling would result in constellation points corrupting each other as different input symbols get mapped to the same symbol after doubling. However, 8PSK can be preserved by tripling. This is illustrated in Fig. 11 [20]. Although the constellation points change their position post-tripling, they do not cause signal corruption. Thus, only certain modulation schemes can be supported with specific multiplication indices in a multiplier-last transmitter [104]. Lastly, bandwidth expansion is a concern due to the non-linear frequency translation in a frequency multiplier (Fig. 11). This can cause the bandwidth occupied by the input baseband signal to expand by N times when passed through a multiply-by-N circuit [20].

It should be noted that the multiplier-last architectures can support 2-level amplitude modulation (such as OOK) without any of the problems mentioned above. This is utilized in [19] to create an efficient THz link at 400 GHz, for instance.

B. Receiver Architectures

At THz frequencies, there exist three commonly used receiver architectures: the low-noise amplifier (LNA)-first architecture (Fig. 12(a)) [103], the mixer-first architecture (Fig. 12(b)) [14]–[16], and the power-detector-based architecture (Fig. 12(c)) [105]. Both LNA-first and mixer-first architectures share similar trade-offs with PA-last and mixer-last architectures. As they are linear, these architectures can accommodate M-QAM modulation schemes. Conversely, the power-detector-based architecture offers a straightforward method for amplitude demodulation while consuming low DC power. Additionally, it can be utilized for phase demodulation by applying a Kramers-Kronig processing technique, as exemplified in [106]. In terms of noise figure, LNA-first architectures offer the lowest, followed by mixer-first architectures. Power-detector-based approaches typically have high noise figures (often exceeding 30 dB) as the conversion gain depends on input received power.

C. Summarizing Remarks

There is no clear conclusion yet on the optimal architecture for THz transceivers. This research remains active, and architectural choices can change with the advent of new techniques, such as heterogeneous integration. However, some initial conclusions can be drawn based on the discussions above.

- If a technology node with a high $f_{\max}$ is used for transceiver design (such as III-V), then a PA-last and LNA-first transceiver, with M-QAM modulation is ideal.
- If such a technology is not available and one is constrained to use a more inferior technology (such as CMOS, SiGe):
  - For high data-rate, short-range links: M-QAM modulation with mixer-last transmitter and mixer-first reciever is optimal. While this can support high data rates, the communication link distance may be limited due to low saturated output power and high noise figure.
  - For moderate to low data-rate, medium-to-long range links: On the transmitter side, a multiplier-last approach is optimal, as it can support high output power. On the receiver end, a mixer-first architecture may be optimal due to its lower noise figure compared to the detector-first approach

VI. ANTENNAS AND PACKAGING

A 300 GHz signal has a wavelength of 1 mm in free space. This enables the design of large antenna arrays within a small area. Moreover, it is important to note that wavelength decreases in a dielectric medium. For example, in silicon dioxide—a widely used dielectric in technologies like silicon CMOS and SiGe BiCMOS—the wavelength of a 300 GHz signal is reduced to just 0.5 mm due to a dielectric constant of 3.9 [111]. This reduction enables the design of a large antenna array within an integrated circuit (IC). For instance, a 144-element on-chip array is demonstrated at 670 GHz in [112].

Efficient antennas and their interfacing methods are crucial for every wireless communication system. In a traditional RF signal chain, the LNA and PA interface with the antenna.

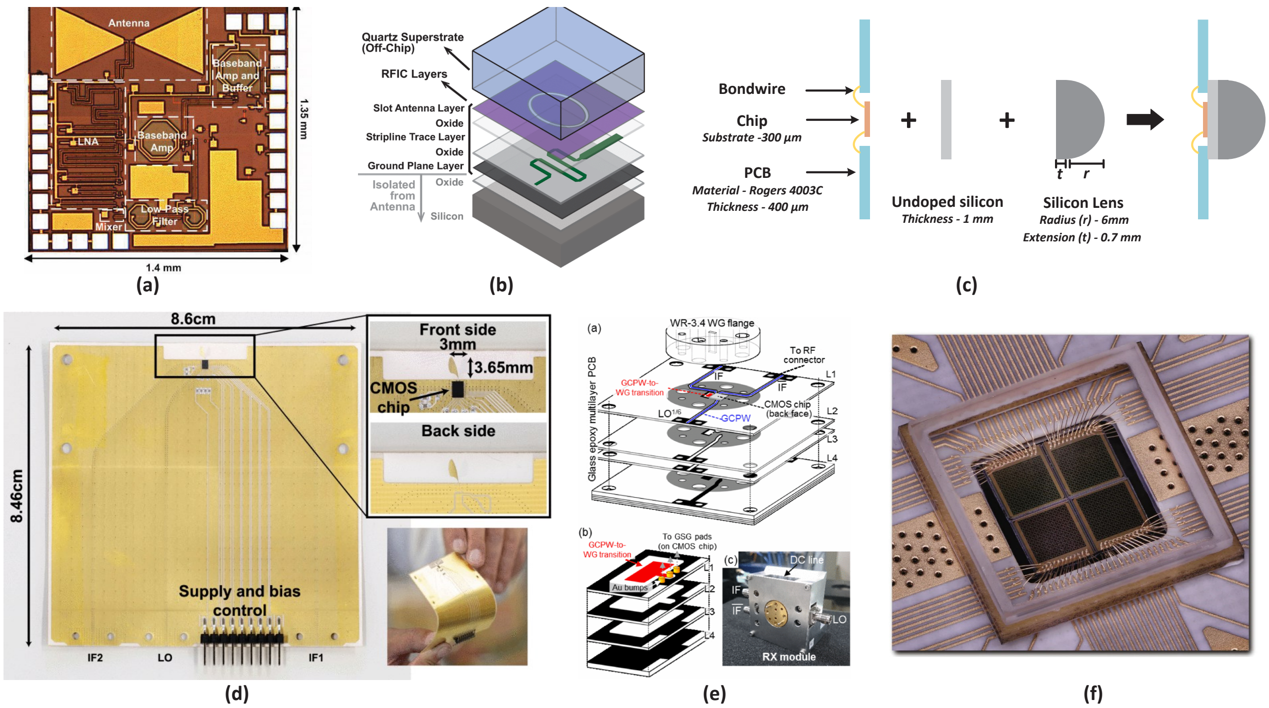

FIGURE 13. (a) An on-chip bowtie antenna implemented in a 130nm SiGe BiCMOS platform [107]. (b) Adding a quartz superstrate to increase the directivity and gain of top-side radiation [108]. (c) Silicon lens packaged to a silicon die [19]. (d) Photographs of the PCB with Vivaldi antennas used for a 300 GHz phased-array [16]. (e) CMOS chip to a waveguide transition built on a multilayered glass epoxy PCB [109]. (f) Four CMOS chips (each measuring 2 mm × 2 m) consisting of a programmable two-dimensional array of 12 × 12 meta-elements [110].

Inefficiencies in the antenna or its interfacing can lead to increased noise figure in the LNA and decreased efficiency and output power in the PA, highlighting the importance of developing high-efficiency antennas and employing low-loss packaging techniques for interfacing [113]. Besides this, packages also need to provide mechanical support and protection from external conditions and facilitate thermal dissipation while providing easy interfacing with DC biases and I/O control signals.

This section explores the latest advancements in antenna design and packaging approaches at THz frequencies. While our primary emphasis is silicon ICs, the techniques and principles discussed apply to a broad spectrum of other semiconductor technologies.

A. Integrated On-Chip Antennas

Given the reduced wavelength in silicon, it is feasible to integrate antennas directly within integrated circuits (ICs typically have a size of a few millimeters). These antennas are often designed in thick top metal layers to mitigate conductive losses. A variety of antenna designs—including dipole, slot, ring, cavity, leaky-wave, and patch antennas—have been successfully implemented on-chip [108], [114]–[116]. For example, Fig. 13(a) demonstrates an on-chip bowtie antenna implemented in a 130nm SiGe BiCMOS platform [107]. These antennas can be designed to radiate from the top or back sides of the IC, leading to different design strategies, which are discussed below.

1) Top-Side Radiation

Antennas that radiate from the top typically exhibit lower efficiencies. This is because of the significant mismatch in intrinsic impedances between the antenna medium (silicon dioxide) and air [111]. An effective strategy to enhance radiation efficiency involves the addition of a quartz superstrate atop the antenna, a technique that has demonstrated improved radiation efficiency [108], as shown in Fig. 13(b). While this method does necessitate some post-fabrication processing, the associated costs are relatively low.

2) Back-Side Radiation

Radiation from the back side generally achieves higher efficiency compared to top-side radiation. This improvement is due to the high dielectric constant of the silicon substrate beneath the silicon dioxide layer, which lowers intrinsic impedance. However, back-radiation faces challenges, as unwanted surface waves can get generated within the silicon substrate. To address this, a hyper-hemispherical silicon lens can be added, which can significantly boost efficiency and directivity [19], [111], [117]. This is demonstrated in Fig. 13(c). Yet, adopting silicon lenses has drawbacks: they are costly and require precise alignment. When utilized with an array, lenses typically suffer from poor performance due to off-axis effects, where the phase center of individual antenna elements does not align with the lens's phase center [118].

Recent advancements have seen the use of 3D-printed Teflon lenses, which offer enhanced directivity owing to the design flexibility afforded by 3D printing in creating optimal lens shapes [119]. Additionally, the exploration of metasurface-based planar lenses represents a growing field of study [120].

B. Antenna on PCB

Antennas can be integrated onto printed circuit boards (PCBs), offering a cost-effective and flexible solution [16], [121]. Fig. 13(d) demonstrates a Vivaldi antenna array at 300 GHz, implemented by stacking PCBs over one another. However, this approach has notable drawbacks. First, connecting the chip to the PCB requires either bond wires or flip-chip packaging using copper bumps. Both methods can adversely affect impedance matching and increase signal loss. Second, the material typically used in PCBs exhibits high loss at THz frequencies, potentially lowering antenna efficiency. Additionally, the manufacturing resolution available at most PCB facilities may not meet the precise requirements for designing antennas at these high frequencies, particularly for those with sub-millimeter dimensions.

C. Micro-Machined Waveguide Antennas

Waveguide antennas are known for their exceptional performance at THz frequencies. However, interfacing these antennas with ICs presents technical challenges. Typically, bond wires or copper bumps are used to deliver the THz signal to an EM coupler, which then excites the waveguide antenna. This is demonstrated in Fig. 13(e). However, achieving consistent impedance matching proves complex in this approach [109], [122]. An alternative strategy involves embedding the EM coupler directly within the IC, enabling it to directly generate the required EM mode for the antenna [114], [115]. Despite the high quality of antennas and interfaces this method yields, it is expensive due to the high costs involved in micro-machining at such fine dimensions.

D. Other Techniques

Dielectric waveguides (DWG) have attracted attention recently, where a low-loss polymeric medium is used to guide electromagnetic waves at THz frequencies. DWGs exhibit low loss and can hence potentially replace fiber in medium-range links [123], [124]. However, it is important to note that DWGs are not strictly a wireless technology since it requires a dielectric channel to guide the EM wave.

Another area of significant interest is the development of reconfigurable intelligent surfaces (RIS). Designing these advanced structures to operate at THz frequencies presents substantial challenges, primarily because conventional switches fail to function at these high frequencies, complicating reconfigurability. Despite this, there have been demonstrations of THz RIS structures such as metasurfaces for holographic projections [110] (Fig. 13(f)) and reflectarrays using 1-bit phase shifters for high-resolution radar [125].

VII. THZ TRANSCEIVER DEMONSTRATIONS

The focus on THz frequencies has been driven by their largely untapped potential, evidenced by practical applications such as the use of frequencies around 120 GHz for data transmission during the Beijing Olympics [126] and the Air Force Research Laboratory's (AFRL) experiments on propagation loss between aircraft using frequencies in the 300 GHz band [127]. These applications, among others, underscore the significant interest and ongoing efforts within the field to overcome the inherent challenges of operating at such high frequencies. This section delves into a few prototype transceivers above 200 GHz developed by both academia and industry. We highlight some notable demos that have successfully demonstrated a complete over-the-air (OTA) wireless link, encompassing both transmitter and receiver components, capable of achieving multi-Gbps transmission rates.

A. Hiroshima University and NTT

Hiroshima University and Nippon Telegraph and Telephone (NTT) have showcased a series of transceivers within the 300 GHz band, using a 40nm CMOS technology platform [13]–[15]. Notably, [14] presents a complete transceiver capable of sustaining a 3 cm OTA link with a data rate of 80 Gbps while achieving an energy efficiency of 22.3 pJ/bit. This transceiver supports advanced modulation schemes, including QPSK, 16QAM, and 64QAM. Note that this prototype does not include a packaged antenna and interfacing. Instead, the OTA link was tested by interfacing the chip with external waveguide horn antennas via waveguide probes.

Further advancements by the same group are detailed in [15], where the authors demonstrate a receiver module that incorporates packaging. In this development, the 40nm CMOS chip is flip-chip bonded onto a PCB and interfaces with waveguide antennas (Fig. 13(e)). This packaged receiver module can achieve 76 Gbps using 16QAM modulation over a 6 cm distance and 4.32 Gbps with QPSK modulation over a 1 meter OTA distance.

B. BiCMOS Transceiver from University of Wuppertal

The study referenced as [18] showcases a BiCMOS transceiver operating at 230 GHz. The transceiver is equipped with on-chip ring antennas and a silicon lens for optimal radiation, while heat-sinking techniques are implemented to regulate thermal performance (Fig. 14(a)). Notably, this transceiver can attain a data transmission rate of 100 Gbps using 16QAM modulation over a 1-meter link while maintaining an energy efficiency of 14 pJ/bit.

C. Beam-Steerable Phased Array from TokyoTech

TokyoTech has successfully showcased beam steering within the 300 GHz band (from 242-280 GHz), utilizing a 65nm CMOS technology platform [16]. The prototype features a CMOS transceiver paired with PCB-based Vivaldi antennas and can support QPSK and 16QAM modulation schemes

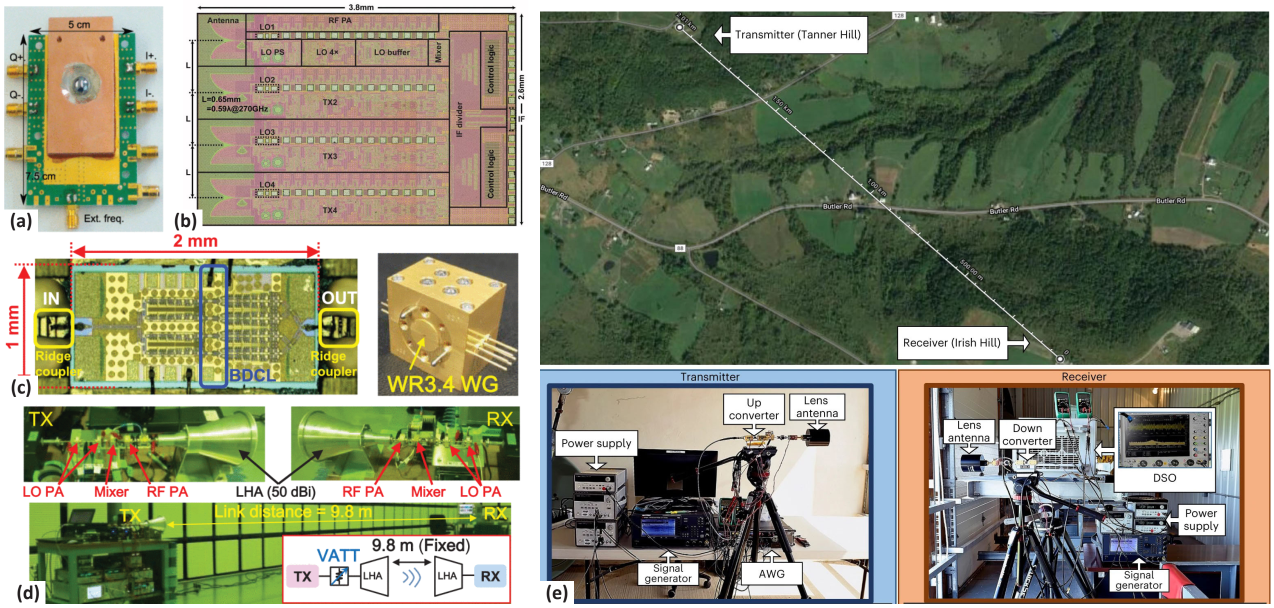

FIGURE 14. (a) 230 GHz BiCMOS transceiver from the University of Wuppertal. The silicon lens and heat-sinking can be observed here [18]. (b) 300 GHz phased array transmitter, with on-chip Vivaldi antenna array IC from TokyoTech [17]. (c) InP power amplifier chip from NTT and TokyoTech with a ridge-coupler and waveguide packaging [103] (d) 300 GHz InP transceiver achieving a 9.8m OTA link [103] (e) A 2 km point-to-point link at the Air Force Research Laboratory research facility, and the corresponding transmitter and receiver hardware [37].

(Fig. 13(d)). By stacking four of these PCBs, the team has managed to electronically steer the beam across a 36-degree span. Furthermore, the design can also operate with standard horn antennas. OTA tests have resulted in data transmission speeds of 16 Gbps over a distance of 3.5 cm while achieving an energy efficiency of 93.75 pJ/bit. Additionally, the team recently demonstrated a new 2-D phased array transmitter by stacking multiple PCBs and chips with on-chip Vivaldi antennas [17] (Fig. 14(b)).

D. NTT and TokyoTech

NTT and TokyoTech have demonstrated a 300 GHz heterodyne transceiver using their in-house 80nm InP HEMT platform [103]. It consists of custom-designed PAs and mixer modules, which are all packaged in individual waveguide modules by using ridge couplers (Fig. 14(c)). Using external high-gain lens antennas, the transceiver achieves OTA data transmission of a 120 Gb/s 16QAM signal over a link distance of 9.8 m (Fig. 14(d)), with an energy efficiency of 92.5 pJ/bit.

E. Multi-Kilometer Link from Northeastern University

Northeastern University has showcased a long-distance, high-speed link at 225 GHz for wireless backhaul [37]. The link supports over 2 Gbps at frequencies between 210–230 GHz across a 2 km OTA outdoor environment, utilizing a 200 mW THz signal source and broadband low-noise balanced mixers employing Schottky diode technology developed by NASA (Fig. 14(e)). The system employs a highly directional lens antenna (with over 40 dBi gain) for the outdoor link setup. It also integrates custom communication and signal processing strategies into a software-defined, ultra-wideband (30 GHz) digital baseband system. It presents cutting-edge outcomes, proving the feasibility of establishing long-distance terahertz links in real-world outdoor settings.

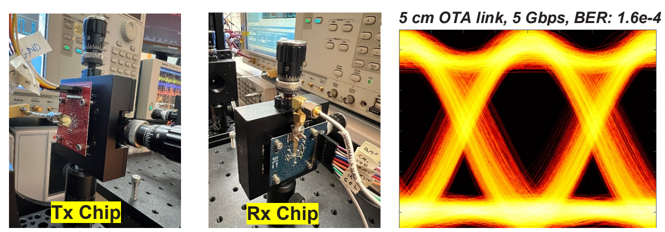

FIGURE 15. 400 GHz transceiver from UCLA and measured eye-diagram for 5 Gbps transmission across a 5 cm OTA link [19].

F. 400 GHz Transceiver from UCLA

UCLA has demonstrated a multi-Gbps wireless transceiver at 400 GHz using a 90nm SiGe BiCMOS process [19]. This work utilizes silicon PIN diodes that show strong non-linearity and can hence generate THz signals with high DC-to-THz generation efficiency. The prototype supports OOK modulation and incorporates on-chip antennas paired with a silicon lens. In OTA experiments, this prototyped transceiver achieved 5 Gb/s of data transmission over a link distance of 5 cm (Fig. 15), with an energy efficiency of 52.8 pJ/bit. Notably, this is the first instance of a fully integrated multi-Gb/s wireless transceiver operating above 300 GHz in silicon. Additionally, by employing external mirrors for collimation, UCLA demonstrated a transmitter that can support 3 Gbps over a 20-meter link [128].

G. Limitations of Current THz Demonstrations

These demonstrations showcase impressive performance, highlighting the feasibility of THz communication. However, they primarily validate feasibility rather than demonstrating a stable, commercially viable product. Many reported demonstrations are conducted in controlled laboratory environments with customized setups, leaving key aspects such as long-term operational reliability across diverse conditions and manufacturing yield—both crucial for commercialization—largely unaddressed. Additionally, many systems rely on large, highly directive antennas that require precise alignment; even slight misalignments can significantly degrade performance, making real-world deployment challenging. This underscores the need for adaptive phased array beamforming and tracking solutions, which have yet to be fully realized at these frequencies.

Furthermore, these demonstrations often fail to account for the energy efficiency of the entire system. For instance, the local oscillator is frequently supplied by an off-chip source, with its power consumption left unreported. Similarly, the power requirements of baseband analog-to-digital conversion blocks are typically overlooked. Moreover, the impressive data rates reported in these studies often depend on extensive equalization performed off-chip, with the associated computational and power costs unaccounted for. Addressing these limitations is essential for the practical realization and large-scale adoption of THz communication systems.

VIII. OPEN RESEARCH AREAS

The development of THz communication presents numerous challenges that require innovative solutions across multiple domains. We outline key open research areas spanning devices, circuits, antennas, and packaging below:

- Process technologies need significant advancements to provide devices with high $f_{\max}$. This can enable the design of energy-efficient THz circuits capable of providing sufficient amplification to overcome the high propagation loss at THz frequencies [81]. Simultaneously, the development of advanced sub-micron CMOS within the same process for the digital back-end is essential [85].
- Heterogeneous integration emerges as a crucial area of exploration to identify ideal devices for specific functions. This also necessitates parallel advancements in packaging technology [87], [95], [96].
- There is a need for novel circuit techniques that can circumvent device limitations and enable circuit design at THz frequencies [112], [129]. Transmitters must deliver high output power with good efficiency, while receivers require amplification with low noise figures [17], [102], [130].
- Realizing analog-to-digital converters, digital-to-analog converters, and baseband processing circuits capable of handling wideband signals remains an understudied yet critical challenge [12]. Signal sampling, an important step in these converters, becomes highly power-consuming due to the wideband nature of the signals. Additionally, maintaining low noise with uniform amplitude and phase response across such wide bandwidths is particularly challenging. Poor performance in these circuits can introduce significant noise and nonlinearities, ultimately degrading the bit-error rate and limiting achievable data rates.
- Equalization techniques need to be implemented on-chip to compensate for frequency-selective fading, multipath effects, and hardware-induced non-idealities. Current demonstrations often rely on off-chip equalization, which introduces additional latency and power consumption [13]–[17].
- High-performance antennas that do not rely on expensive post-processing or precise machining and can work with reasonable manufacturing tolerances are essential for THz systems [113]. 3D-printed Teflon lenses, which offer good design flexibility and cost efficiency, are being actively explored [119]. Additionally, metasurface-based planar lenses represent a promising field of research [120], [131].
- There is significant potential in leveraging the highly directional nature and unique propagation characteristics of THz links for physical layer security, using techniques such as OAM multiplexing and frequency-selective absorption [46], [47], [132].
- Like in mmWave, fast yet reliable beam management and initial access will be essential to deploy robust THz communication systems at scale, especially in mobile and standalone settings. Techniques harnessing emerging technologies such as artificial intelligence and reconfigurable surfaces are showing promise in this pursuit [77]–[80], but there remains the need for real-world experimentation in realistic scenarios to confirm such techniques at THz frequencies. Other techniques, such as wavefront engineering [75], [133], are also proving to be promising directions warranting future investigation for overcoming the propagation characteristics exhibited at THz.

IX. CONCLUSION

The potential to transform wireless communication by operating at THz carrier frequencies has spawned research and development across the globe, with eyes set on enabling future 6G networks. In this survey, we provide a comprehensive overview of recent advancements in THz-based 6G networks, with particular emphasis on the IEEE 802.15.3d standard. We examine key enabling technologies across devices, circuits, antennas, and packaging while highlighting critical areas requiring further research and development. We also highlight notable experimental demonstrations of THz-based 6G networks worldwide. Finally, we outline several open research areas that must be addressed to advance the field.

While there has been significant progress in the field in recent years, notable shortcomings related to cost, energy efficiency, and reliability remain, which must be addressed for practical deployment. Despite these practical hurdles, the global enthusiasm for THz communication raises hope that it will become a core component in revolutionizing future generations of connectivity.

As THz technology continues to evolve, a holistic approach that accounts for technical, environmental, and societal considerations will be essential for its responsible development and deployment. Investigating the potential long-term biological effects of THz radiation and ensuring that its integration does not interfere with critical radio astronomy and Earth observation satellites remain pressing concerns. Furthermore, advanced THz sensing capabilities, such as JCAS, necessitate stringent security and privacy measures to mitigate potential misuse. Equally important is the need to bridge the existing digital divide by ensuring equitable access to these advancements. Addressing these multifaceted challenges will be crucial in realizing the transformative potential of THz technology in future communication systems.

REFERENCES

[1] T. S. Rappaport, Y. Xing, O. Kanhere, S. Ju, A. Madanayake, S. Mandal, A. Alkhateeb, and G. C. Trichopoulos, "Wireless communications and applications above 100 GHz: opportunities and challenges for 6G and beyond," *IEEE Access*, vol. 7, pp. 78 729–78 757, 2019.
[2] S. Dang, O. Amin, B. Shihada, and M.-S. Alouini, "What should 6G be?" *Nature Electronics*, vol. 3, no. 1, pp. 20–29, 2020.
[3] T. Barnett, S. Jain, U. Andra, and T. Khurana, "Cisco visual networking index (VNI) complete forecast update, 2017-2022," *Americas/EMEAR Cisco Knowledge Network (CKN) Presentation*, pp. 1–30, 2018.
[4] U. Cisco, "Cisco annual internet report (2018–2023) white paper," *Cisco: San Jose, CA, USA*, vol. 10, no. 1, pp. 1–35, 2020.
[5] Ericsson. (2023, October) 6G network architecture – a proposal for early alignment. https://www.ericsson.com/en/reports-and-papers/ericsson-technology-review/articles/6g-network-architecture.
[6] Int. Telecommun.Union, ITU-Recommedation, "IMT traffic estimates for the years 2020 to 2030," vol. M.2370, no. 0, 2015.
[7] M. Z. Chowdhury, M. Shahjalal, S. Ahmed, and Y. M. Jang, "6G wireless communication systems: Applications, requirements, technologies, challenges, and research directions," *IEEE Open Journal of the Communications Society*, vol. 1, pp. 957–975, 2020.
[8] M. Giordani, M. Polese, M. Mezzavilla, S. Rangan, and M. Zorzi, "Toward 6G networks: Use cases and technologies," *IEEE Communications Magazine*, vol. 58, no. 3, pp. 55–61, 2020.
[9] J. M. Jornet, E. W. Knightly, and D. M. Mittleman, "Wireless communications sensing and security above 100 GHz," *Nature communications*, vol. 14, no. 1, p. 841, 2023.
[10] S. Li, Z. Zhang, B. Rupakula, and G. M. Rebeiz, "An eight-element 140-GHz wafer-scale IF beamforming phased-array receiver with 64-QAM operation in CMOS RFSOI," *IEEE Journal of Solid-State Circuits*, vol. 57, no. 2, pp. 385–399, 2022.
[11] M. Elkhouly, J. Ha, M. J. Holyoak, D. Hendry, M. Sayginer, R. Enright, I. Kimionis, Y. Baeyens, and S. Shahramian, "Fully integrated 2D scalable tx/rx chipset for D-band phased-array-on-glass modules," in *2022 IEEE International Solid-State Circuits Conference (ISSCC)*, vol. 65, 2022, pp. 76–78.
[12] A. Agrawal, A. Whitcombe, W. Shin, R. Bhat, S. Kundu, P. Sagazio, H. Chandrakumar, T. W. Brown, B. R. Carlton, C. Hull, S. Callender, and S. Pellerano, "A 128-gb/s d-band receiver with integrated pll and adc achieving 1.95-pj/b efficiency in 22-nm finfet," *IEEE Journal of Solid-State Circuits*, vol. 58, no. 12, pp. 3364–3379, 2023.
[13] K. Katayama, K. Takano, S. Amakawa, S. Hara, A. Kasamatsu, K. Mizuno, K. Takahashi, T. Yoshida, and M. Fujishima, "A 300 GHz CMOS transmitter with 32-QAM 17.5 Gb/s/ch capability over six channels," *IEEE Journal of Solid-State Circuits*, vol. 51, no. 12, pp. 3037–3048, 2016.
[14] S. Lee, S. Hara, T. Yoshida, S. Amakawa, R. Dong, A. Kasamatsu, J. Sato, and M. Fujishima, "An 80-Gb/s 300-GHz-band single-chip CMOS transceiver," *IEEE Journal of Solid-State Circuits*, vol. 54, no. 12, pp. 3577–3588, 2019.
[15] S. Hara, R. Dong, S. Lee, K. Takano, N. Toshida, A. Kasamatsu, K. Sakakibara, T. Yoshida, S. Amakawa, and M. Fujishima, "A 76-Gbit/s 265-GHz CMOS receiver with WR-3.4 waveguide interface," *IEEE Journal of Solid-State Circuits*, vol. 57, no. 10, pp. 2988–2998, 2022.
[16] I. Abdo, C. da Gomez, C. Wang, K. Hatano, Q. Li, C. Liu, K. Yanagisawa, A. A. Fadila, T. Fujimura, T. Miura, K. K. Tokgoz, J. Pang, H. Hamada, H. Nosaka, A. Shirane, and K. Okada, "A bi-directional 300-ghz-band phased-array transceiver in 65-nm cmos with outphasing transmitting mode and LO emission cancellation," *IEEE Journal of Solid-State Circuits*, vol. 57, no. 8, pp. 2292–2308, 2022.
[17] C. Wang, H. Herdian, W. Zheng, C. Liu, J. Mayeda, Y. Liu, O. A. Yong, W. Wang, Y. Zhang, C. D. Gomez, A. Shehata, S. Kato, I. Abdo, T. Jyo, H. Hamada, H. Takahashi, H. Sakai, A. Shirane, and K. Okada, "24.3 a 236-to-266 GHz 4-element amplifier-last phased-array transmitter in 65nm CMOS," in *2024 IEEE International Solid-State Circuits Conference (ISSCC)*, vol. 67, 2024, pp. 415–417.
[18] P. Rodríguez-Vázquez, J. Grzyb, B. Heinemann, and U. R. Pfeiffer, "A 16-QAM 100-Gb/s 1-m wireless link with an EVM of 17% at 230 GHz in an SiGe technology," *IEEE Microwave and Wireless Components Letters*, vol. 29, no. 4, pp. 297–299, 2019.
[19] S. Thomas, S. Razavian, J. S. Virdi, W. Sun, B. F. Motlagh, and A. Babakhani, "A 400-GHz efficient radiator and OOK transceiver for multi-Gb/s wireless communication in silicon," *IEEE Journal of Solid-State Circuits*, pp. 1–17, 2024.
[20] A. Standaert and P. Reynaert, "A 390-GHz outphasing transmitter in 28-nm CMOS," *IEEE Journal of Solid-State Circuits*, vol. 55, no. 10, pp. 2703–2713, 2020.
[21] H.-J. Song and N. Lee, "Terahertz communications: Challenges in the next decade," *IEEE Transactions on Terahertz Science and Technology*, vol. 12, no. 2, pp. 105–117, 2022.
[22] I. F. Akyildiz, C. Han, Z. Hu, S. Nie, and J. M. Jornet, "Terahertz band communication: An old problem revisited and research directions for the next decade," *IEEE Transactions on Communications*, vol. 70, no. 6, pp. 4250–4285, 2022.
[23] I. F. Akyildiz, J. M. Jornet, and C. Han, "Terahertz band: Next frontier for wireless communications," *Physical communication*, vol. 12, pp. 16–32, 2014.
[24] H. Elayan, O. Amin, B. Shihada, R. M. Shubair, and M.-S. Alouini, "Terahertz band: The last piece of RF spectrum puzzle for communication systems," *IEEE Open Journal of the Communications Society*, vol. 1, pp. 1–32, 2020.
[25] S. Razavian, S. Thomas, M. Hosseini, and A. Babakhani, "Micro-doppler detection and vibration sensing using silicon-based thz radiators," *IEEE Sensors Journal*, vol. 22, no. 14, pp. 14 091–14 101, 2022.
[26] A. Mostajeran, H. Aghasi, S. M. H. Naghavi, and E. Afshari, "Fully integrated solutions for high resolution terahertz imaging (invited)," in *2019 IEEE Custom Integrated Circuits Conference (CICC)*, 2019, pp. 1–8.
[27] M. Tonouchi, "Cutting-edge terahertz technology," *Nature photonics*, vol. 1, no. 2, pp. 97–105, 2007.
[28] A. Goldsmith, *Wireless communications*. Cambridge university press, 2005.
[29] T. S. Rappaport, S. Sun, R. Mayzus, H. Zhao, Y. Azar, K. Wang, G. N. Wong, J. K. Schulz, M. Samimi, and F. Gutierrez, "Millimeter wave mobile communications for 5G cellular: It will work!" *IEEE Access*, vol. 1, pp. 335–349, 2013.

[30] "F3: The path to 6G: Architectures, circuits, technologies for sub-thz communications, sensing and imaging," in *2022 IEEE International Solid-State Circuits Conference (ISSCC)*, vol. 65, 2022, pp. 534–536.

[31] N. Rajatheva, I. Atzeni, E. Bjornson, A. Bourdoux, S. Buzzi, J.-B. Dore, S. Erkucuk, M. Fuentes, K. Guan, Y. Hu *et al.*, "White paper on broadband connectivity in 6G," *arXiv preprint arXiv:2004.14247*, 2020.

[32] D. C. Nguyen, M. Ding, P. N. Pathirana, A. Seneviratne, J. Li, D. Niyato, O. Dobre, and H. V. Poor, "6G internet of things: A comprehensive survey," *IEEE Internet of Things Journal*, vol. 9, no. 1, pp. 359–383, 2022.

[33] H.-J. Song, H. Hamada, and M. Yaita, "Prototype of kiosk data downloading system at 300 GHz: Design, technical feasibility, and results," *IEEE Communications Magazine*, vol. 56, no. 6, pp. 130–136, 2018.

[34] C. Cookson, "Time is money when it comes to microwaves," *Financial Times*, vol. 10, 2013.

[35] M. Cudak, A. Ghosh, A. Ghosh, and J. G. Andrews, "Integrated access and backhaul: A key enabler for 5G millimeter-wave deployments," *IEEE Communications Magazine*, vol. 59, no. 4, pp. 88–94, Apr. 2021.

[36] M. Polese, M. Giordani, T. Zugno, A. Roy, S. Goyal, D. Castor, and M. Zorzi, "Integrated access and backhaul in 5G mmWave networks: Potential and challenges," *IEEE Communications Magazine*, vol. 58, no. 3, pp. 62–68, Mar. 2020.

[37] P. Sen, J. V. Siles, N. Thawdar, and J. M. Jornet, "Multi-kilometre and multi-gigabit-per-second sub-terahertz communications for wireless backhaul applications," *Nature Electronics*, vol. 6, no. 2, pp. 164–175, 2023.

[38] A. Alkhateeb, S. Jiang, and G. Charan, "Real-time digital twins: Vision and research directions for 6g and beyond," *IEEE Communications Magazine*, vol. 61, no. 11, pp. 128–134, 2023.

[39] X. Xu, Y. Pan, P. P. M. Y. Lwin, and X. Liang, "3D holographic display and its data transmission requirement," in *2011 International Conference on Information Photonics and Optical Communications*, 2011, pp. 1–4.

[40] Q. Zhang, J. Liu, and G. Zhao, "Towards 5g enabled tactile robotic telesurgery," *arXiv preprint arXiv:1803.03586*, 2018.

[41] V. Petrov, T. Kurner, and I. Hosako, "IEEE 802.15.3d: First standardization efforts for sub-terahertz band communications toward 6G," *IEEE Communications Magazine*, vol. 58, no. 11, pp. 28–33, 2020.

[42] D. M. Pozar, *Microwave engineering*. John wiley & sons, 2011.

[43] T. Wild, V. Braun, and H. Viswanathan, "Joint design of communication and sensing for beyond 5G and 6G systems," *IEEE Access*, vol. 9, pp. 30 845–30 857, 2021.

[44] Ericsson. (2021, October) Joint sensing and communication: The foundation of 6G. https://www.ericsson.com/en/blog/2021/10/joint-sensing-and-communication-6g.

[45] T. S. Rappaport, R. W. Heath Jr, R. C. Daniels, and J. N. Murdock, *Millimeter wave wireless communications*. Pearson Education, 2015.

[46] S. Venkatesh, H. Saeidi, K. Sengupta, and X. Lu, "Millimeter-wave physical layer security through space-time modulated transmitter arrays," in *2022 IEEE 22nd Annual Wireless and Microwave Technology Conference (WAMICON)*, 2022, pp. 1–4.

[47] M. I. W. Khan, J. Woo, X. Yi, M. I. Ibrahim, R. T. Yazicigil, A. P. Chandrakasan, and R. Han, "A 0.31-thz orbital-angular-momentum (OAM) wave transceiver in CMOS with bits-to-OAM mode mapping," *IEEE Journal of Solid-State Circuits*, vol. 57, no. 5, pp. 1344–1357, 2022.

[48] W. Sun, S. Thomas, and A. Babakhani, "A 360 ghz single-element multi-mode orbital angular momentum cavity antenna-based transmitter in 90nm sige bicmos," in *2024 IEEE Radio Frequency Integrated Circuits Symposium (RFIC)*, 2024, pp. 331–334.

[49] J. Y. Suen, "Terabit-per-second satellite links: A path toward ubiquitous terahertz communication," *Journal of Infrared, Millimeter, and Terahertz Waves*, vol. 37, no. 7, pp. 615–639, 2016.

[50] I. Mehdi, J. Siles, C. P. Chen, and J. M. Jornet, "THz technology for space communications," in *2018 Asia-Pacific Microwave Conference (APMC)*, 2018, pp. 76–78.

[51] N. Lu, N. Cheng, N. Zhang, X. Shen, and J. W. Mark, "Connected vehicles: Solutions and challenges," *IEEE Internet of Things Journal*, vol. 1, no. 4, pp. 289–299, 2014.

[52] K. Tekbıyık, A. R. Ekti, G. K. Kurt, and A. Görçin, "Terahertz band communication systems: Challenges, novelties and standardization efforts," *Physical Communication*, vol. 35, p. 100700, 2019.

[53] Z. Chen, X. Ma, B. Zhang, Y. Zhang, Z. Niu, N. Kuang, W. Chen, L. Li, and S. Li, "A survey on terahertz communications," *China Communications*, vol. 16, no. 2, pp. 1–35, 2019.

[54] Y. He, Y. Chen, L. Zhang, S.-W. Wong, and Z. N. Chen, "An overview of terahertz antennas," *China Communications*, vol. 17, no. 7, pp. 124–165, 2020.

[55] F. Lemic, S. Abadal, W. Tavernier, P. Stroobant, D. Colle, E. Alarcón, J. Marquez-Barja, and J. Famaey, "Survey on terahertz nanocommunication and networking: A top-down perspective," *IEEE Journal on Selected Areas in Communications*, vol. 39, no. 6, pp. 1506–1543, 2021.

[56] C.-X. Wang, J. Wang, S. Hu, Z. H. Jiang, J. Tao, and F. Yan, "Key technologies in 6g terahertz wireless communication systems: A survey," *IEEE Vehicular Technology Magazine*, vol. 16, no. 4, pp. 27–37, 2021.

[57] C. Han, Y. Wang, Y. Li, Y. Chen, N. A. Abbasi, T. Kürner, and A. F. Molisch, "Terahertz wireless channels: A holistic survey on measurement, modeling, and analysis," *IEEE Communications Surveys & Tutorials*, vol. 24, no. 3, pp. 1670–1707, 2022.

[58] D. Serghiou, M. Khalily, T. W. C. Brown, and R. Tafazolli, "Terahertz channel propagation phenomena, measurement techniques and modeling for 6g wireless communication applications: A survey, open challenges and future research directions," *IEEE Communications Surveys Tutorials*, vol. 24, no. 4, pp. 1957–1996, 2022.

[59] W. Jiang, Q. Zhou, J. He, M. A. Habibi, S. Melnyk, M. El-Absi, B. Han, M. D. Renzo, H. D. Schotten, F.-L. Luo, T. S. El-Bawab, M. Juntti, M. Debbah, and V. C. M. Leung, "Terahertz communications and sensing for 6g and beyond: A comprehensive review," *IEEE Communications Surveys Tutorials*, pp. 1–1, 2024.

[60] Federal Communications Commission. (2024, September) Fcc online table of frequency allocations. https://www.fcc.gov/engineering-technology/policy-and-rules-division/radio-spectrum-allocation/general/table-frequency.

[61] European Telecommunications Standards Institute. (2019) ETSI TR 103 498 V1.1.1 (2019-02). https://www.etsi.org/deliver/etsi_tr/103400_103499/103498/01.01.01_60/tr_103498v010101p.pdf.

[62] "802.15.3d-2017 - IEEE standard for high data rate wireless multi-media networks–amendment 2: 100 gb/s wireless switched point-to-point physical layer," *IEEE Std 802.15.3d-2017 (Amendment to IEEE Std 802.15.3-2016 as amended by IEEE Std 802.15.3e-2017)*, pp. 1–55, 2017.

[63] P. Series, "Attenuation by atmospheric gases and related effects," *Recommendation ITU-R*, vol. 25, pp. 676–12, 2019.

[64] I. E. Gordon, L. S. Rothman, R. Hargreaves, R. Hashemi, E. V. Karlovets, F. Skinner, E. K. Conway, C. Hill, R. V. Kochanov, Y. Tan *et al.*, "The HITRAN2020 molecular spectroscopic database," *Journal of quantitative spectroscopy and radiative transfer*, vol. 277, p. 107949, 2022.

[65] M. M. Assefzadeh, B. Jamali, A. K. Gluszek, A. J. Hudzikowski, J. Wojtas, F. K. Tittel, and A. Babakhani, "Terahertz trace gas spectroscopy based on a fully-electronic frequency-comb radiating array in silicon," in *2016 Conference on Lasers and Electro-Optics (CLEO)*, 2016, pp. 1–2.

[66] T. S. Rappaport, *Wireless communications: principles and practice*. Cambridge University Press, 2024.

[67] S. Ju, S. H. A. Shah, M. A. Javed, J. Li, G. Palteru, J. Robin, Y. Xing, O. Kanhere, and T. S. Rappaport, "Scattering mechanisms and modeling for terahertz wireless communications," in *ICC 2019 - 2019 IEEE International Conference on Communications (ICC)*, 2019, pp. 1–7.

[68] M. Rodwell, "Sub-mm-wave technologies: Systems, ICs, THz transistors," in *2013 Asia-Pacific Microwave Conference Proceedings (APMC)*. IEEE, 2013, pp. 509–511.

[69] C. A. Balanis, *Antenna theory: analysis and design*. John wiley & sons, 2016.

[70] H. Sarieddeen, M.-S. Alouini, and T. Y. Al-Naffouri, "An overview of signal processing techniques for terahertz communications," *Proceedings of the IEEE*, vol. 109, no. 10, pp. 1628–1665, 2021.

[71] A. Faisal, H. Sarieddeen, H. Dahrouj, T. Y. Al-Naffouri, and M.-S. Alouini, "Ultramassive MIMO systems at terahertz bands: Prospects

and challenges," *IEEE Vehicular Technology Magazine*, vol. 15, no. 4, pp. 33–42, 2020.

[72] B. Govind, T. Tapen, and A. Apsel, "Ultra-compact quasi-true time delay for boosting wireless channel capacity," *Nature*, vol. 627, no. 8002, pp. 88–94, 2024.

[73] X. Fu, F. Yang, C. Liu, X. Wu, and T. J. Cui, "Terahertz beam steering technologies: from phased arrays to field-programmable metasurfaces," *Advanced optical materials*, vol. 8, no. 3, p. 1900628, 2020.

[74] R. Xu, S. Gao, B. S. Izquierdo, C. Gu, P. Reynaert, A. Standaert, G. J. Gibbons, W. Bösch, M. E. Gadringer, and D. Li, "A review of broadband low-cost and high-gain low-terahertz antennas for wireless communications applications," *Ieee Access*, vol. 8, pp. 57 615–57 629, 2020.

[75] H. Guerboukha, B. Zhao, Z. Fang, E. Knightly, and D. M. Mittleman, "Curving thz wireless data links around obstacles," *Communications Engineering*, vol. 3, no. 1, pp. 1–8, 2024.

[76] Y. Heng, J. G. Andrews, J. Mo, V. Va, A. Ali, B. L. Ng, and J. C. Zhang, "Six key challenges for beam management in 5.5G and 6G systems," *IEEE Wireless Communications Magazine*, vol. 59, no. 7, pp. 74–79, Jul. 2021.

[77] Q. Xue, C. Ji, S. Ma, J. Guo, Y. Xu, Q. Chen, and W. Zhang, "A survey of beam management for mmwave and thz communications towards 6g," *IEEE Communications Surveys Tutorials*, vol. 26, no. 3, pp. 1520–1559, 2024.

[78] W. Attaoui, K. Bouraqia, and E. Sabir, "Initial access beam alignment for mmwave and terahertz communications," *IEEE Access*, vol. 10, pp. 35 363–35 397, 2022.

[79] M. Qurratulain Khan, A. Gaber, P. Schulz, and G. Fettweis, "Machine learning for millimeter wave and terahertz beam management: A survey and open challenges," *IEEE Access*, vol. 11, pp. 11 880–11 902, 2023.

[80] J. A. Zhang, M. L. Rahman, K. Wu, X. Huang, Y. J. Guo, S. Chen, and J. Yuan, "Enabling joint communication and radar sensing in mobile networks—a survey," *IEEE Communications Surveys Tutorials*, vol. 24, no. 1, pp. 306–345, 2022.

[81] K. Sengupta, T. Nagatsuma, and D. M. Mittleman, "Terahertz integrated electronic and hybrid electronic-photonic systems," *Nature Electronics*, vol. 1, no. 12, pp. 622–635, 2018.

[82] K. Sengupta, "Integrated circuits for terahertz communication beyond 100 GHz: are we there yet?" in *2019 IEEE International Conference on Communications Workshops (ICC Workshops)*, 2019, pp. 1–6.

[83] E. Seok, D. Shim, C. Mao, R. Han, S. Sankaran, C. Cao, W. Knap, and K. K. O, "Progress and challenges towards terahertz CMOS integrated circuits," *IEEE Journal of Solid-State Circuits*, vol. 45, no. 8, pp. 1554–1564, 2010.

[84] C. Doan, S. Emami, A. Niknejad, and R. Brodersen, "Millimeter-wave CMOS design," *IEEE Journal of Solid-State Circuits*, vol. 40, no. 1, pp. 144–155, 2005.

[85] B. Nauta, "1.2 racing down the slopes of moore's law," in *2024 IEEE International Solid-State Circuits Conference (ISSCC)*, vol. 67, 2024, pp. 16–23.

[86] X. Mei, W. Yoshida, M. Lange, J. Lee, J. Zhou, P.-H. Liu, K. Leong, A. Zamora, J. Padilla, S. Sarkozy, R. Lai, and W. R. Deal, "First demonstration of amplification at 1 THz using 25-nm InP high electron mobility transistor process," *IEEE Electron Device Letters*, vol. 36, no. 4, pp. 327–329, 2015.

[87] A. Gutierrez-Aitken, "Heterogeneous integration for high frequency RF applications," in *2020 IEEE International Electron Devices Meeting (IEDM)*. IEEE, 2020, pp. 34–5.

[88] S. Ong, L. Chan, K. Chew, C. Lim, W. L. Oo, A. Bellaouar, C. Zhang, W. Chow, T. Chen, R. Rassel, J. Wong, C. Wan, J. Kim, W. Seet, and D. Harame, "22nm FD-SOI technology with back-biasing capability offers excellent performance for enabling efficient, ultra-low power analog and RF/millimeter-wave designs," in *2019 IEEE Radio Frequency Integrated Circuits Symposium (RFIC)*, 2019, pp. 323–326.

[89] B. Heinemann, H. Rücker, R. Barth, F. Bärwolf, J. Drews, G. G. Fischer, A. Fox, O. Fursenko, T. Grabolla, F. Herzel, J. Katzer, J. Korn, A. Krüger, P. Kulse, T. Lenke, M. Lisker, S. Marschmeyer, A. Scheit, D. Schmidt, J. Schmidt, M. A. Schubert, A. Trusch, C. Wipf, and D. Wolansky, "SiGe HBT with f_T/f_{max} of 505 GHz/720 GHz," in *2016 IEEE International Electron Devices Meeting (IEDM)*, 2016, pp. 3.1.1–3.1.4.

[90] J. Pekarik, V. Jain, C. Kenney, J. Holt, S. Khokale, S. Saroop, J. B. Johnson, K. Stein, V. Ontalus, C. Durcan, M. Nafari, T. Nesheiwat, S. Saudari, E. Yarmoghaddam, S. Chaurasia, and A. Joseph, "SiGe HBTs with $f_T/f_{\max} \sim 375/510GHz$ integrated in 45nm PDSOI CMOS," in *2021 IEEE BiCMOS and Compound Semiconductor Integrated Circuits and Technology Symposium (BCICTS)*, 2021, pp. 1–4.

[91] R. Lai, X. Mei, W. Deal, W. Yoshida, Y. Kim, P. Liu, J. Lee, J. Uyeda, V. Radisic, M. Lange *et al.*, "Sub 50 nm InP HEMT device with fmax greater than 1 THz," in *2007 IEEE international electron devices meeting*. IEEE, 2007, pp. 609–611.

[92] M. Urteaga, Z. Griffith, M. Seo, J. Hacker, and M. J. Rodwell, "InP HBT technologies for THz integrated circuits," *Proceedings of the IEEE*, vol. 105, no. 6, pp. 1051–1067, 2017.

[93] DARPA. (2020) T-MUSIC proposer's day. https://www.darpa.mil/attachments/T-MUSIC_Proposers%20Day_Jan30.pdf.

[94] European Commission. (2017) TARANTO. https://cordis.europa.eu/project/id/737454.

[95] J. Li, Y. Royter, P. Patterson, T. Hussain, J. Duvall, M. Montes, D. Le, D. Hitko, M. Sokolich, D. Chow, and K. Elliott, "Heterogeneous wafer-scale integration of 250nm, 300GHz InP DHBTs with a 130nm RF-CMOS technology," in *2008 IEEE International Electron Devices Meeting*, 2008, pp. 1–3.

[96] M. Urteaga, A. Carter, Z. Griffith, R. Pierson, J. Bergman, A. Arias, P. Rowell, J. Hacker, B. Brar, and M. Rodwell, "THz bandwidth InP HBT technologies and heterogeneous integration with Si CMOS," in *2016 IEEE Bipolar/BiCMOS Circuits and Technology Meeting (BCTM)*, 2016, pp. 35–41.

[97] D. Cimbri, J. Wang, A. Al-Khalidi, and E. Wasige, "Resonant tunneling diodes high-speed terahertz wireless communications - a review," *IEEE Transactions on Terahertz Science and Technology*, vol. 12, no. 3, pp. 226–244, 2022.

[98] R. Basu, L. R. Billa, R. Letizia, and C. Paoloni, "Design of sub-THz traveling wave tubes for high data rate long range wireless links," *Semiconductor Science and Technology*, vol. 33, no. 12, p. 124009, 2018.

[99] B. S. Williams, "Terahertz quantum-cascade lasers," *Nature photonics*, vol. 1, no. 9, pp. 517–525, 2007.

[100] S. Voinigescu, *High-frequency integrated circuits*. Cambridge University Press, 2013.

[101] O. Momeni and E. Afshari, "A broadband mm-wave and terahertz traveling-wave frequency multiplier on CMOS," *IEEE Journal of Solid-State Circuits*, vol. 46, no. 12, pp. 2966–2976, 2011.

[102] S. Ghosh, F. Zhang, H. Guo, and K. K. O, "305-GHz cascode power amplifier using capacitive feedback fabricated using SiGe HBT's with fmax of 450 GHz," in *2023 IEEE Radio Frequency Integrated Circuits Symposium (RFIC)*, 2023, pp. 313–316.

[103] H. Hamada, T. Tsutsumi, H. Matsuzaki, T. Fujimura, I. Abdo, A. Shirane, K. Okada, G. Itami, H.-J. Song, H. Sugiyama, and H. Nosaka, "300-GHz-band 120-Gb/s wireless front-end based on InP-HEMT PAs and mixers," *IEEE Journal of Solid-State Circuits*, vol. 55, no. 9, pp. 2316–2335, 2020.

[104] S. Kang, S. V. Thyagarajan, and A. M. Niknejad, "A 240 GHz fully integrated wideband QPSK transmitter in 65 nm CMOS," *IEEE Journal of Solid-State Circuits*, vol. 50, no. 10, pp. 2256–2267, 2015.

[105] Z. Wang, P.-Y. Chiang, P. Nazari, C.-C. Wang, Z. Chen, and P. Heydari, "A CMOS 210-GHz fundamental transceiver with OOK modulation," *IEEE Journal of Solid-State Circuits*, vol. 49, no. 3, pp. 564–580, 2014.

[106] S. Ghozzy, M. Allam, E. A. Karahan, Z. Liu, and K. Sengupta, "12.2 a mm-wave/sub-THz synthesizer-free coherent receiver with phase reconstruction through mixed-signal kramer-kronig processing," in *2024 IEEE International Solid-State Circuits Conference (ISSCC)*, vol. 67, 2024, pp. 220–222.

[107] H. Aggrawal, P. Chen, M. M. Assefzadeh, B. Jamali, and A. Babakhani, "Gone in a picosecond: Techniques for the generation and detection of picosecond pulses and their applications," *IEEE Microwave Magazine*, vol. 17, no. 12, pp. 24–38, 2016.

[108] J. M. Edwards and G. M. Rebeiz, "High-efficiency elliptical slot antennas with quartz superstrates for silicon RFICs," *IEEE Transactions on Antennas and Propagation*, vol. 60, no. 11, pp. 5010–5020, 2012.

[109] S. Hara, K. Takano, K. Katayama, R. Dong, K. Mizuno, K. Takahashi, I. Watanabe, N. Sekine, A. Kasamatsu, T. Yoshida, S. Amakawa, and M. Fujishima, "300-GHz CMOS receiver module with WR-3.4

waveguide interface," in *2018 48th European Microwave Conference (EuMC)*, 2018, pp. 396–399.
[110] S. Venkatesh, X. Lu, H. Saeidi, and K. Sengupta, "A high-speed programmable and scalable terahertz holographic metasurface based on tiled CMOS chips," *Nature electronics*, vol. 3, no. 12, pp. 785–793, 2020.
[111] A. Babakhani, "Direct antenna modulation (DAM) for on-chip mm-wave transceivers," Ph.D. dissertation, California Institute of Technology, 2008.
[112] L. Gao and C. H. Chan, "24.1 a 0.64-to-0.69 THz beam-steerable coherent source with 9.1 dBm radiated power and 30.8dBm lensless EIRP in 65nm CMOS," in *2023 IEEE International Solid-State Circuits Conference (ISSCC)*, 2023, pp. 362–364.
[113] H.-J. Song, "Packages for terahertz electronics," *Proceedings of the IEEE*, vol. 105, no. 6, pp. 1121–1138, 2017.
[114] W. R. Deal, X. B. Mei, V. Radisic, K. Leong, S. Sarkozy, B. Gorospe, J. Lee, P. H. Liu, W. Yoshida, J. Zhou, M. Lange, J. Uyeda, and R. Lai, "Demonstration of a 0.48 THz amplifier module using InP HEMT transistors," *IEEE Microwave and Wireless Components Letters*, vol. 20, no. 5, pp. 289–291, 2010.
[115] L. Samoska, W. R. Deal, G. Chattopadhyay, D. Pukala, A. Fung, T. Gaier, M. Soria, V. Radisic, X. Mei, and R. Lai, "A submillimeter-wave HEMT amplifier module with integrated waveguide transitions operating above 300 ghz," *IEEE Transactions on Microwave Theory and Techniques*, vol. 56, no. 6, pp. 1380–1388, 2008.
[116] H. Saeidi, S. Venkatesh, X. Lu, and K. Sengupta, "THz prism: One-shot simultaneous localization of multiple wireless nodes with leaky-wave thz antennas and transceivers in CMOS," *IEEE Journal of Solid-State Circuits*, vol. 56, no. 12, pp. 3840–3854, 2021.
[117] T. Tajima, H.-J. Song, and M. Yaita, "Compact THz LTCC receiver module for 300 GHz wireless communications," *IEEE Microwave and Wireless Components Letters*, vol. 26, no. 4, pp. 291–293, 2016.
[118] D. Filipovic, G. Gauthier, S. Raman, and G. Rebeiz, "Off-axis properties of silicon and quartz dielectric lens antennas," *IEEE Transactions on Antennas and Propagation*, vol. 45, no. 5, pp. 760–766, 1997.
[119] L. Gao and C. H. Chan, "A 0.45-THz 2-D scalable radiator array with 28.2-dBm EIRP using an elliptical teflon lens," *IEEE Journal of Solid-State Circuits*, vol. 57, no. 2, pp. 400–412, 2022.
[120] J. Zhu, Y. Yang, M. Li, D. McGloin, S. Liao, J. Nulman, M. Yamada, and F. Iacopi, "Additively manufactured millimeter-wave dual-band single-polarization shared aperture fresnel zone plate metalens antenna," *IEEE Transactions on Antennas and Propagation*, vol. 69, no. 10, pp. 6261–6272, 2021.
[121] O. Koutsos, F. F. Manzillo, M. Caillet, R. Sauleau, and A. Clemente, "Experimental demonstration of a 43-dBi gain transmit array in PCB technology for backhauling in the 300-GHz band," *IEEE Transactions on Terahertz Science and Technology*, vol. 13, no. 5, pp. 485–492, 2023.
[122] A. Tessmann, A. Leuther, V. Hurm, H. Massler, M. Zink, M. Kuri, M. Riessle, R. Losch, M. Schlechtweg, and O. Ambacher, "A 300 GHz mHEMT amplifier module," in *2009 IEEE International Conference on Indium Phosphide Related Materials*, 2009, pp. 196–199.
[123] P. Reynaert, M. Tytgat, W. Volkaerts, A. Standaert, Y. Zhang, M. De Wit, and N. Van Thienen, "Polymer microwave fibers: A blend of RF, copper and optical communication," in *ESSCIRC Conference 2016: 42nd European Solid-State Circuits Conference*, 2016, pp. 15–20.
[124] J. W. Holloway, G. C. Dogiamis, and R. Han, "11.9 a 105Gb/s dielectric-waveguide link in 130nm BiCMOS using channelized 220-to-335 GHz signal and integrated waveguide coupler," in *2021 IEEE International Solid-State Circuits Conference (ISSCC)*, vol. 64, 2021, pp. 196–198.
[125] N. M. Monroe, G. C. Dogiamis, R. Stingel, P. Myers, X. Chen, and R. Han, "Electronic THz pencil beam forming and 2D steering for high angular-resolution operation: A 98 $\times$ 98-unit 265 GHz CMOS reflectarray with in-unit digital beam shaping and squint correction," in *2022 IEEE International Solid-State Circuits Conference (ISSCC)*, vol. 65, 2022, pp. 1–3.
[126] A. Hirata, "Transmission trial of television broadcast materials using 120-GHz-band wireless link," *NTT Tech. Rev.*, vol. 7, no. 3, 2009.
[127] Air Force Research Laboratory. (2023) AFRL conducts first flight experiments for communications in terahertz band. https://www.afrl.af.mil/News/Article-Display/Article/3348325/afrl-conducts-first-flight-experiments-for-communications-in-terahertz-band/.
[128] S. Razavian, S. Thomas, M. Hosseini, and A. Babakhani, "A 0.4 THz efficient OOK/FSK wireless transmitter enabling 3 Gbps at 20 meters," in *2022 IEEE BiCMOS and Compound Semiconductor Integrated Circuits and Technology Symposium (BCICTS)*, 2022, pp. 178–181.
[129] S. Thomas, S. Razavian, W. Sun, B. F. Motlagh, A. D. Kim, Y. Wu, B. S. Williams, and A. Babakhani, "A 0.4-4 thz p-i-n diode frequency multiplier in 90-nm sige bicmos," *IEEE Journal of Solid-State Circuits*, vol. 58, no. 9, pp. 2407–2420, 2023.
[130] S. P. Singh, T. Rahkonen, M. E. Leinonen, and A. Parssinen, "Design aspects of single-ended and differential sige low-noise amplifiers operating above fmax/2in sub-thz/thz frequencies," *IEEE Journal of Solid-State Circuits*, vol. 58, no. 9, pp. 2478–2488, 2023.
[131] G.-B. Wu, J. Y. Dai, K. M. Shum, K. F. Chan, Q. Cheng, T. J. Cui, and C. H. Chan, "A universal metasurface antenna to manipulate all fundamental characteristics of electromagnetic waves," *Nature Communications*, vol. 14, no. 1, p. 5155, 2023.
[132] W. Sun, S. Thomas, and A. Babakhani, "Fully integrated multimode orbital angular momentum wave generation at 360 ghz using sige bicmos," *IEEE Transactions on Microwave Theory and Techniques*, pp. 1–12, 2025.
[133] A. Singh, V. Petrov, H. Guerboukha, I. V. Reddy, E. W. Knightly, D. M. Mittleman, and J. M. Jornet, "Wavefront engineering: Realizing efficient terahertz band communications in 6g and beyond," *IEEE Wireless Communications*, vol. 31, no. 3, pp. 133–139, 2024.

Sidharth Thomas (S'20) received the B.Tech. degree in Electronics and Communication Engineering from Indian Institute of Technology Roorkee in 2020 and the M.S. degree in electrical and computer engineering from University of California, Los Angeles, CA, USA, in 2022, where he is currently pursuing a Ph.D. degree. He was a mm-Wave IC Design Intern with Texas Instruments, Dallas, in 2023. He interned at Intel Labs, Hillsboro, in 2024. His research interests include high-frequency integrated circuit design for wireless communication, imaging, and sensing applications. He received the IIT Roorkee ECE Dept. Gold Medal in 2020, the IEEE MTT-S Pre-Graduate/Graduate Fellowship in 2022, and the 2023–2024 IEEE Solid-State Circuits Society Predoctoral Achievement award.

Jaskirat Singh Virdi (S'23) received his B.Tech. in Electronics and Communication Engineering from the Indian Institute of Technology (IIT) Roorkee, Roorkee, India in 2020. He is currently pursuing a Ph.D. degree in Electrical Engineering at the University of California, Los Angeles, CA, USA. During his undergraduate studies, he was an analog design intern at Texas Instruments Inc., Bangalore, India in 2019, where he worked on bi-directional I/O circuits. He later joined Texas Instruments Inc., Bangalore, India as a full-time analog design engineer and worked on several analog circuits from 2020 to 2021. His current research focuses on multi-Gb/s wireless transceivers and THz/mm-wave integrated circuits (ICs) for various applications like communication and sensing. Mr. Virdi received the UCLA Electrical Engineering Department fellowship in 2021.

Aydin Babakhani (M'08) received the B.S. degree from the Sharif University of Technology, Tehran, Iran, in 2003, and the M.S. and Ph.D. degrees in electrical engineering from the California Institute of Technology, Pasadena, CA, USA, in 2005 and 2008, respectively. From 2011 to 2016, he was an Assistant Professor of electrical and computer engineering, and from 2016 to 2017, he was a Louis Owen Junior Chair Assistant Professor with Rice University, Houston, TX, USA. He was a Post-Doctoral Scholar with the California Institute of Technology in 2009. He was a Research Scientist with the IBM Thomas J. Watson Research Center, Ossining, NY, USA, in 2010. He was an Associate Professor with the Department of Electrical and Computer Engineering, Rice University, where he is currently the Director of the Rice Integrated Systems and Circuits Laboratory. He is also a member of DARPA Microsystems Exploratory Council and a co-founder of MicroSilicon, Inc. He is currently an associate Professor with the Department of Electrical and Computer Engineering, University of California at Los Angeles (UCLA), Los Angeles, CA, USA, where he is also the Director of the Integrated Sensors Laboratory. He has authored or coauthored more than 85 articles in peer-reviewed journals and conference proceedings. He holds 21 issued or pending patents. Dr. Babakhani was a recipient of multiple Best Paper Awards, including the Best Paper Award at the IEEE SiRF Conference in 2016, the Best Paper Award at the IEEE RWS Symposium in 2015, the Best Paper Award at the IEEE MTT-S IMS Symposium in 2014, and Second Place in the Best Paper Awards at the IEEE APS Symposium 2016 and IEEE MTT-S IMS Symposium 2016. His research is supported by NSF, DARPA, AFOSR, ONR, the W. M. Keck Foundation, SRC, and more than ten companies. He was also a recipient of the prestigious NSF CAREER Award in 2015, an Innovation Award from Northrop Grumman in 2014, a DARPA Young Faculty Award in 2012, the California Institute of Technology Electrical Engineering Department's Charles Wilts Best Ph.D. Thesis Prize for his work entitled "Near-Field Direct Antenna Modulation," the Microwave Graduate Fellowship in 2007, the Grand Prize in the Stanford-Berkeley-Caltech Innovators Challenge in 2006, the Analog Devices, Inc., Outstanding Student Designer Award in 2005, the California Institute of Technology Special Institute Fellowship, and an Atwood Fellowship in 2003. He was also a recipient of the Gold Medal Winner at both the National Physics Competition in 1998 and the 30th International Physics Olympiad, Padua, Italy, in 1999.

Ian P. Roberts (M'23) received the B.S. degree in electrical engineering from the Missouri University of Science and Technology and the M.S. and Ph.D. degrees in electrical and computer engineering from the University of Texas at Austin, where he was a National Science Foundation Graduate Research Fellow with the Wireless Networking and Communications Group. He is currently an assistant professor of electrical and computer engineering at the University of California, Los Angeles (UCLA). He has industry experience developing and prototyping wireless technologies at AT&T Labs, Amazon, GenXComm (startup), and Sandia National Labs. His research interests are in the theory and implementation of mmWave/THz systems, in-band full-duplex, and other next-generation technologies for wireless communication and sensing. He is an associate editor for the IEEE Open Journal of the Communications Society. In 2023, he received the Andrea Goldsmith Young Scholars Award from the Communication Theory Technical Committee of the IEEE Communications Society.